doi:10.1093/brain/aws323 Brain 2013: 136; 223–244 | 223

BRAIN
A JOURNAL OF NEUROLOGY

New insights into genotype–phenotype correlations for the doublecortin-related lissencephaly spectrum

Nadia Bahi-Buisson,[1,2,3] Isabelle Souville,[4] Franck J. Fourniol,[5] Aurelie Toussaint,[4] Carolyn A. Moores,[5] Anne Houdusse,[6] Jean Yves Lemaitre,[7] Karine Poirier,[2,3] Reham Khalaf-Nazzal,[8,9,10] Marie Hully,[1] Pierre Louis Leger,[1] Caroline Elie,[11] Nathalie Boddaert,[7,12] Cherif Beldjord,[4] Jamel Chelly,[2,3] Fiona Francis[8,9,10] and SBH-LIS European Consortium[†]

1 Neurologie pédiatrique, Hopital Necker Enfants Malades, Université Paris Descartes, APHP, Paris, France
2 Institut Cochin, Université Paris-Descartes, CNRS (UMR 8104), Paris, France
3 INSERM U1016, Paris, France
4 Biologie Moléculaire et Génétique, Hôpital Cochin, AP-HP, Université Paris Descartes, Paris, France
5 Institute of Structural Molecular Biology, Birkbeck College, London
6 Motilité Structurale, Institut Curie CNRS, UMR 144, Paris, France
7 INSERM U1000 'Imagerie et Psychiatrie', INSERM-CEA-Faculté de Médecine, Paris Sud 11, France
8 INSERM UMR-S839, F75005, Paris, France
9 Universite Pierre et Marie Curie, F75005, Paris, France
10 Institut du Fer à Moulin, F75005, Paris, France
11 Biostatistics Hopital Necker Enfants Malades, Université Paris Descartes, APHP, Paris, France
12 Radiologie Pédiatrique, Hopital Necker Enfants Malades, Université Paris Descartes, APHP, Paris, France

[†]SBH-LIS European consortium listed in Appendix 1

Correspondence to: Nadia Bahi-Buisson, MD, PhD,
Pediatric Neurology Hopital Necker Enfants Malades,
Université Paris Descartes,
APHP,
149 rue de Sevres 75015 Paris,
France
E-mail: nadia.bahi-buisson@nck.aphp.fr

X-linked isolated lissencephaly sequence and subcortical band heterotopia are allelic human disorders associated with mutations of *doublecortin* (*DCX*), giving both familial and sporadic forms. DCX encodes a microtubule-associated protein involved in neuronal migration during brain development. Structural data show that mutations can fall either in surface residues, likely to impair partner interactions, or in buried residues, likely to impair protein stability. Despite the progress in understanding the molecular basis of these disorders, the prognosis value of the location and impact of individual *DCX* mutations has largely remained unclear. To clarify this point, we investigated a cohort of 180 patients who were referred with the agyria–pachygyria subcortical band heterotopia spectrum. *DCX* mutations were identified in 136 individuals. Analysis of the parents' DNA revealed the *de novo* occurrence of *DCX* mutations in 76 cases [62 of 70 females screened (88.5%) and 14 of 60 males screened (23%)], whereas in the remaining cases, mutations were inherited from asymptomatic ($n = 14$) or symptomatic mothers ($n = 11$). This represents 100% of families screened. Female patients with *DCX* mutation demonstrated three degrees of clinical–radiological severity: a severe form with a thick band ($n = 54$), a milder form ($n = 24$) with either an anterior thin or an intermediate thickness band and asymptomatic carrier females ($n = 14$) with normal magnetic resonance imaging results. A higher proportion of

Received May 24, 2012. Revised October 20, 2012. Accepted October 22, 2012

nonsense and frameshift mutations were identified in patients with *de novo* mutations. An analysis of predicted effects of missense mutations showed that those destabilizing the structure of the protein were often associated with more severe phenotypes. We identified several severe- and mild-effect mutations affecting surface residues and observed that the substituted amino acid is also critical in determining severity. Recurrent mutations representing 34.5% of all *DCX* mutations often lead to similar phenotypes, for example, either severe in sporadic subcortical band heterotopia owing to Arg186 mutations or milder in familial cases owing to Arg196 mutations. Taken as a whole, these observations demonstrate that *DCX*-related disorders are clinically heterogeneous, with severe sporadic and milder familial subcortical band heterotopia, each associated with specific *DCX* mutations. There is a clear influence of the individual mutated residue and the substituted amino acid in determining phenotype severity.

Keywords: band heterotopia; lissencephaly; doublecortin; microtubules

Abbreviation: SBH = subcortical band heterotopia

Introduction

Genetically inherited disorders of neuronal migration represent important causes of epilepsy and intellectual disability. Subcortical band heterotopia (SBH), also known as 'double cortex' syndrome, is a neuronal migration disorder characterized by ribbons of grey matter within the central white matter between the cortex and the ventricular surface. The gyral pattern ranges from normal to simplified, with broad convolutions, and cortical thickness is often increased (Barkovich *et al*., 1994; Dobyns *et al*., 1996). Together, SBH and lissencephaly comprise a spectrum of malformations associated with deficient neuronal migration that are caused by alterations in at least three genes: *LIS1* (also known as *PAFAH1B1*) (Reiner *et al*., 1993; Lo Nigro *et al*., 1997), *DCX* (des Portes *et al*., 1998*a*; Gleeson *et al*., 1998) and alpha 1 tubulin (also known as *TUBA1A*) (Keays *et al*., 2007; Poirier *et al*., 2007). Mutations in other tubulin genes (*TUBB2B*, *TUBA8* and *TUBB3)* were also reported in malformations of cortical development, usually polymicrogyria with microcephaly (Abdollahi *et al*., 2009; Jaglin *et al*., 2009; Poirier *et al*., 2010; Tischfield *et al*., 2010).

Patients with SBH have a variable clinical course ranging from mildly to severely impaired. The brain malformation is often revealed by onset of seizures within the first decade. These usually evolve to refractory and multifocal epilepsy. Neurological examination is normal in most cases, but hypotonia, poor fine motor control and behavioural disturbances may be present (Barkovich *et al*., 1989, 1994). Clinical severity varies with the cortical abnormalities, the band thickness and the degree of ventricular enlargement (Palmini *et al*., 1991; Barkovich *et al*., 1994). Patients with correlated pachygyria, thicker heterotopic bands, and severe ventricular enlargement have worse prognoses for neuromotor development. Additionally, they have earlier seizure onset and develop symptomatic generalized epilepsy that resembles Lennox–Gastaut syndrome. Additionally, periventricular and subcortical white matter T_2 hypersignals are correlated with delayed motor development (Barkovich *et al*., 1994).

Most cases with SBH are females, and at least 100 SBH cases have been previously reported (des Portes *et al*., 1998*a*, *b*; Gleeson *et al*., 1998, 1999*a*, 2000*a*; Pilz *et al*., 1998; Dobyns *et al*., 1999; Aigner *et al*., 2000, 2003; Demelas *et al*., 2001; Matsumoto *et al*., 2001; Poolos *et al*., 2002; Guerrini *et al*., 2003; Mei *et al*., 2007; Haverfield *et al*., 2009). Although most patients are sporadic, a syndrome of familial SBH with X-linked inheritance has been described in which the majority of females have SBH and affected males usually present isolated lissencephaly with more severe abnormalities over anterior brain regions (Pilz *et al*., 1998; Dobyns *et al*., 1999; Gleeson *et al*., 2000*a*). *DCX* mutations cause SBH in heterozygous carrier females and lissencephaly in hemizygous males (des Portes *et al*., 1998*a*; Gleeson *et al*., 1998; Pilz *et al*., 1998), although rare males with SBH and mosaic *DCX* mutations have been reported (Pilz *et al*., 1999; Guerrini *et al*., 2003). *DCX* mutations have been found in all familial cases and in 53% (Gleeson *et al*., 2000) to 84% (Matsumoto *et al*., 2001) of patients with SBH. The frequency of mutations in the most common forms of sporadic SBH is ~80% of cases (Matsumoto *et al*., 2001). Recently, large genomic deletions and duplications were also found to account for a proportion of unexplained cases (Mei *et al*., 2007; Haverfield *et al*., 2009).

The DCX protein is the best described member of a family of neuronal microtubule-associated proteins that are involved in cell division and/or cell migration (Gleeson *et al*., 1998). DCX is expressed in migrating and differentiating neurons; it is centrally involved in organizing the microtubule cytoskeleton, and this function is essential for neuronal migration (Francis *et al*., 1999; Gleeson *et al*., 1999*b*; Kappeler *et al*., 2006; Koizumi *et al*., 2006). The DCX microtubule binding domain is made up of two DC (doublecortin-homology) domains, namely an N-terminal (N-DC; amino acids 46–139) and a C-terminal (C-DC; amino acids 173–263) domain. Lissencephaly-causing missense mutations mainly cluster within these tandem DC domains, supporting the significance of microtubule binding for DCX function (Sapir *et al*., 2000; Taylor *et al*., 2000). In contrast, nonsense mutations occur randomly throughout the protein. The N-DC domain can directly bind to microtubules (Kim *et al*., 2003), whereas the C-DC domain has also been implicated in binding free tubulin and other cellular partners (Caspi *et al*., 2000; Kizhatil *et al*., 2002; Tsukada *et al*., 2003; Friocourt *et al*., 2005). DCX binds at an unusual site on the microtubule lattice (Moores *et al*., 2004, 2006). This confers specificity for microtubule architecture so that DCX preferentially nucleates and stabilizes 13-protofilament microtubules, the *in vivo* microtubule architecture (Tilney *et al*., 1973).

The availabilities of the 3D structure of N-DC of DCX (Kim *et al*., 2003) and C-DC of DCDC2 (2DNF.PDB in the protein databank) and a subnanometer-resolution structure of DCX interacting with microtubules (Fourniol *et al*., 2010) has allowed us to predict the impact of disease-causing point mutations on DCX function. Mutations in buried sites are likely to lead to a loss or a reduction in stability, while mutation of surface residues can influence interactions with microtubules or other binding partners. Although a small number of mutations were previously evaluated structurally (Kim *et al*., 2003), here we have analysed *DCX* mutations from a unique and large European cohort of 136 patients, including 25 families. Overall, we present data for 93 females with SBH and compare these with the corresponding features in 43 males. To better define the phenotypic spectrum, brain MRI and the clinical phenotype of patients were characterized. Using clinical, imaging molecular and structural data in combination with X-inactivation studies where possible, we provide new insights into genotype–phenotype correlations for the *DCX*-related lissencephaly spectrum.

Materials and methods

Patients selection

As part of our ongoing lissencephaly and cortical malformation collection, 180 patients with agyria–pachygyria–SBH spectrum were referred to our laboratory for molecular screening (APHP-Cochin Hospital). This cohort included 70 females with sporadic SBH, 46 patients from 18 families (with either two brothers with lissencephaly, two sisters with SBH or affected mothers with SBH and a son with lissencephaly, or foetal male cases with lissencephaly) and 60 males with sporadic lissencephaly. Patients included were from 20 centres in France, Israel and Switzerland. All patients were known personally to at least one of the authors.

Mutation analysis

Clinical data and blood samples were obtained with informed consent from patients, and DNA was extracted using a standard protocol. Mutation analysis of the coding sequence of *DCX* (RefSeq NM_00119553) and *LIS1* was performed in all patients as described previously (des Portes *et al*., 1998*a*). DNA samples of the parents were screened in all cases. Mutation detection was performed by direct sequencing of genomic DNA, and if negative, by multiplex ligation-dependent probe amplification (MLPA) analysis combined with single multiplex semi-quantitative fluorescent PCR analysis to validate MLPA findings as described previously (Mei *et al*., 2007). The investigators were unaware of the mutation detected at the time of initial review of the neuroimaging data. The mutations for pedigrees 9, 11 and 15 have been reported previously, and the patients were re-evaluated for this study and were referred to as Families 1, 3 and 2, respectively (des Portes *et al*., 1998*a*, *b*). Mutations for sporadic patients DCX_SBH_46, DCX_SBH_82, DCX_SBH_83 and DCX_SBH_86 were also described previously and referred to as Cases O.D, J.A, B.T and M.L, respectively (des Portes *et al*., 1998*b*).

X-inactivation studies were performed using the androgen receptor–specific HpaII/PCR assay, described elsewhere, to assess X-inactivation patterns (Collins and Jukes, 1994; Monteiro *et al*., 1998). X-inactivation patterns were classified as random (ratio 50:50 < 75:25) or skewed (ratio > 75:25).

Clinical review

Detailed information regarding family history, pre- and perinatal events, age of seizure onset, psychomotor development, cognitive function and neurological examination was collected. Protocols were approved by the appropriate institutional review board committee.

A revised terminology was used for classification of seizures and epileptic syndromes (Berg *et al*., 2010). Levels of cognitive function were graded based on available clinical information. When IQ had not been tested, cognitive function was estimated by using adaptive behavioural criteria.

Brain imaging studies

Magnetic resonance images were available for all patients, were reviewed independently by two of the authors (N.B. and N.B.B.) and classified using previously developed rating scales that were further modified for this study (Dobyns *et al*., 1999). Magnetic resonance images were analysed for the degree of pachygyria (number of gyri and depth of sulci), location of the band and the presence of other brain anomalies. For statistical analyses, lissencephaly was graded according to the following patterning scale, referred to as the Dobyns lissencephaly grade (LIS grade). Grades 1–6 denote the overall severity as seen on neuroimaging, with LIS grade 1 being the most severe (complete agyria) and LIS grade 6 being the least severe (SBH). Bands were graded as previously described (Barkovich *et al*., 1994). Band thickness was graded 1 (<4 mm at the thickest point), 2 (4–7 mm), 3 (8–10 mm) or 4 (>12 mm). Sulcal pattern was graded from normal to overt pachygyria, and additional abnormalities were also recorded.

Volumetric analysis

Structural MRIs of patients with SBH were segmented into grey matter, white matter and CSF maps using Statistical Parametric Mapping (SPM8, http://www.fil.ion.ucl.ac.uk/spm/software/spm8/) and VBM8 toolbox (http://dbm.neuro.uni-jena.de/vbm/). Grey matter probability maps were multiplied by the SPM white matter prior map to give more weight to the grey matter present in the subcortical band. These SBH-weighted maps were thresholded to a height threshold of 50% and an extent threshold of 4 cm^3. Total grey matter and subcortical band volumes were then computed for each patient from the entire grey matter map and the thresholded SBH-weighted map, respectively.

Statistical analysis

Age differences between different groups were analysed using the Kruskal–Wallis rank sum test. Differences in neurological symptoms, cognitive function, behavioural disturbances, imaging characteristics of the SBH and presence of additional brain abnormalities were analysed using χ^2 square test or Fisher's exact test, as appropriate.

Structural analysis

Atomic structures were visualized and docked into the subnanometre-resolution cryo-electron microscopy reconstruction of the DCX–microtubule interface using UCSF Chimera (Pettersen *et al*., 2004). To build the potential C-DC–microtubule interface, a homology model of DCX

C-DC (residues 179–263) was generated with MODELLER (Sali and Blundell, 1993) based on the atomic structure of the DCDC2 C-DC domain (2DNF.PDB; 32% sequence identity with DCX C-DC). Missing residues forming the linker N-terminal to C-DC (residues 174–178) were modelled and moved manually into the cryo-electron microscopy reconstruction using UCSF Chimera.

Results

DCX mutations

As part of our ongoing diagnosis of patients and families with the lissencephaly–SBH spectrum, *DCX* mutations were identified in 62 of 70 females with sporadic SBH (88.5%), in 46 patients from 18 families with lissencephaly–SBH (representing all familial cases) and in 21 of 60 males with the apparently sporadic lissencephaly condition (35%), although seven were subsequently found to have inherited *DCX* mutations from asymptomatic female carrier mothers and were subsequently considered as 'familial cases'.

Distinct mutations were found in females and males (Figs 1 and 2). Among the 83 apparently sporadic cases with *DCX* mutations, analysis of the parents' DNA revealed the *de novo* occurrence of mutations in 76 cases (62 females and 14 males). Fifty-nine different *DCX* mutations were identified *de novo*; of these, 24 were novel, and 14 were detected several times in unrelated patients (Tables 1 and 2).

Forty-five different *DCX* mutations were found in 62 females with sporadic SBH; there were either missense (26/45; 58%), nonsense (7/45; 15.6%), frameshift (8/45; 17.8%) with insertion or deletion of one or two base pairs leading to premature protein termination, splice site mutations (3/45; 6.7%) or deletion of exon 1–2 (1/45; 2.2%). Most missense mutations (24/26; 92.3%) were distributed between N-DC (13/24; 54.2%) and C-DC (11/24; 45.8%) (Fig. 1 and Table 1). Two additional missense mutations fell in the linkers p.A33P in the N-terminal linker upstream of N-DC, and p.V177G in the N-DC-C-DC interdomain linker. Interestingly, several recurrent mutations defining potential hot spots were found, the most frequent being mutations affecting Arg186 (p.R186C, p.R186H or p.R186L) observed in 13 females (20.9%) (Fig. 1). Other recurrent missense (p.R78C, p.R78H, p.R78L or p.R192W) or nonsense (p.R39X or p.R303X) mutations were found in 2–3 cases each. Altogether, these hot spot mutations represent 38.7% of *de novo DCX* SBH mutations. Males with true sporadic lissencephaly carried 14 different *de novo DCX* mutations, that were never found in sporadic females with SBH or inherited SBH/LIS conditions (13/14), except for one splice mutation (c.705 + 1 G > A) that was also identified in one female (Figs 1 and 2, Table 2). Most were missense mutations (8/13), clustered in C-DC (5/8) and in N-DC (3/8). Others were frameshift in one case (c.403_404delAA p.K135fsX164) and an in-frame insertion–deletion (c.560_568del8insTGGTTACCATCATC) in the C-DC domain in another. Finally, three additional patients harboured mosaic mutations: nonsense mutations in the N- (p.R19X) and C- (p.R303X) terminal linkers and a deletion encompassing *DCX* exon 6, respectively.

Twenty inherited *DCX* mutations were identified in 60 individuals from 25 families (see Supplementary Fig. 1 and Figs 1 and 2). These comprised 11 families (25 individuals, 15 females and 10 males) in whom the mother presented with SBH and seven families (21 individuals, 9 females and 12 males) in whom the mother was asymptomatic with either two affected sons ($n = 5$) or two female cousins ($n = 1$), or two brothers whose mother's DNA and clinical data were not available ($n = 1$). The remaining seven families (14 individuals, 7 females and 7 males) were initially referred for sporadic lissencephaly in males, and the asymptomatic mother was subsequently diagnosed with a *DCX* mutation. Most carried missense mutations ($n = 16$) with two recurrent mutations affecting Asp62 and Arg196. Missense mutations were located either in the N terminal or the interdomain linker (4/16), in N-DC (4/16) or in C-DC (8/16). The remaining were nonsense (p.R272X), or affecting the first methionine of *DCX* (c.2T > C; pMet1?), or converting the stop codon into a Phe residue, leading to 48 extra amino acids (c.1144T > A; p.X361PheX48), or an in-frame deletion of exons 3 and 4, and a duplication of exons 4–7 (Table 1 and Supplementary Table 1, Supplementary Fig. 1).

Notably, the majority of mutations identified in asymptomatic mothers were different from those detected in sporadic SBH and more interestingly in symptomatic mothers. Moreover, we identified a recurrent mutation located in Arg196 (p.R196C, p.R196H) found in four asymptomatic carrier females and their sons ($n = 5$), representing 4 of 14 inherited mutations with asymptomatic mothers (Figs 1 and 2). Finally, in 10 female carriers, we had the opportunity to screen for *DCX* mutations in grandmothers. Notably, 9 of 10 female carriers (including two symptomatic and seven asymptomatic patients) harboured *de novo* mutations. Only one asymptomatic mother carried a mutation (p.T42P) inherited from her asymptomatic mother. One of two asymptomatic female carriers carrying the mutation p.D9N showed skewed X-inactivation but had a daughter without neurological symptoms and without any bias, suggesting that this mutation also has a mild effect on DCX function.

The patients for whom *DCX* screening was negative were tested for *LIS1* mutations. Of these, two females and two males were found with mosaic *LIS1* mutations and were therefore not included here.

Skewed X-inactivation (>75%) was found in 6 of 16 tested female carriers (three symptomatic and three asymptomatic) compared with 6 of 38 tested patients with sporadic SBH ($P = 0.15$). While the majority of *DCX* mutations are different between patients with *de novo* and inherited mutations, two mutations (i.e. p.R272X and p.R192W) were found in both groups (des Portes *et al.*, 1998*a*, *b*). For both mutations, skewed inactivation accounts for the clinical variability. Also of note are p.Y125H (inherited) and p.Y125D (*de novo*) mutations because although both were associated with severe phenotypes in children, neither clinical nor X-inactivation data were available to explain a presumed milder phenotype in the transmitting female.

Clinical and radiological presentation of patients with subcortical band heterotopia and outcome

The SBH cohort comprised 62 females with *de novo* mutations and 16 cases with inherited mutations (10 symptomatic female

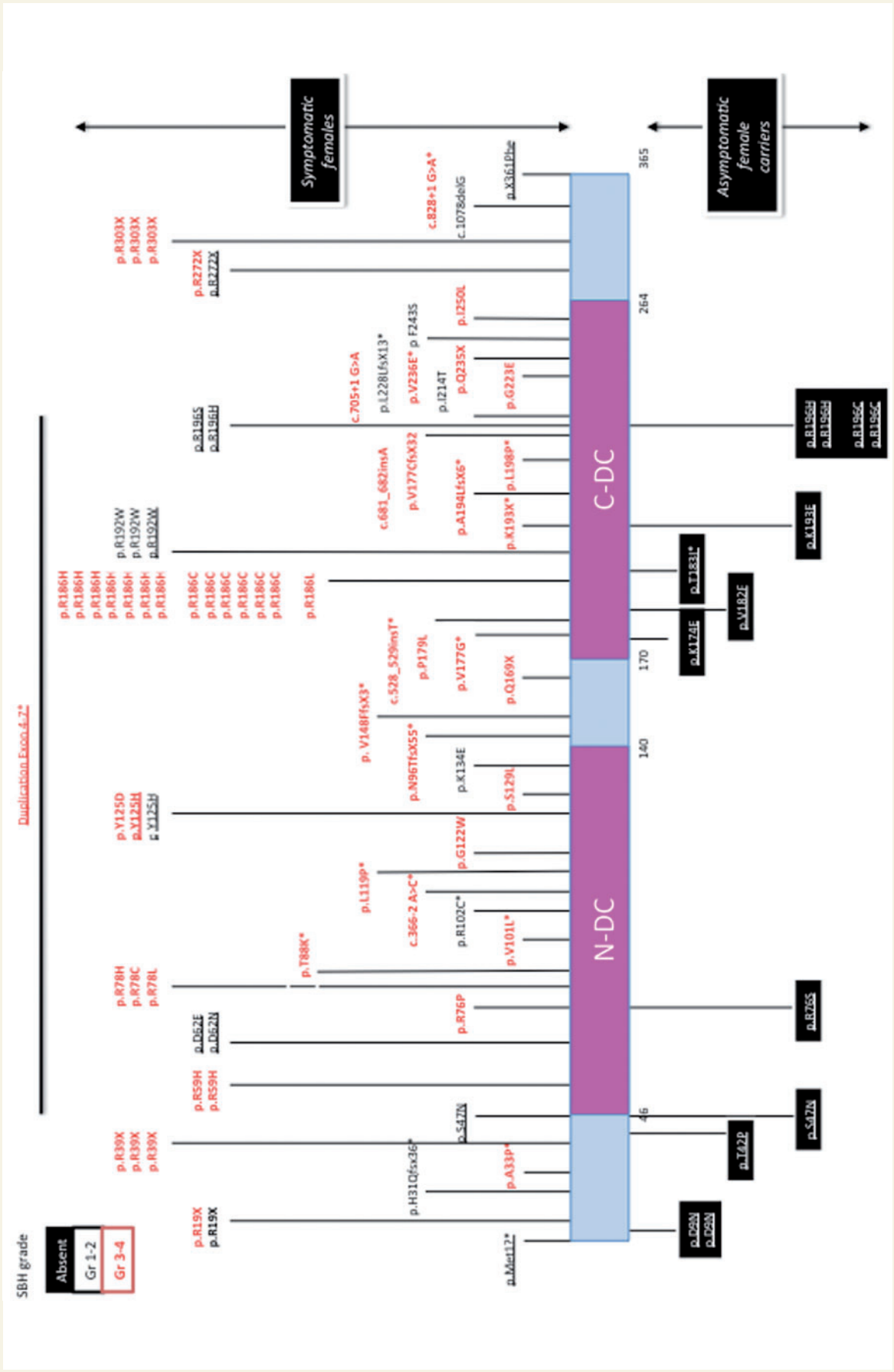

Figure 1 Schematic representation of the DCX protein and summary of the mutations identified in asymptomatic and symptomatic females with SBH. Each *DCX* nucleotide mutation is numbered with reference to the ATG. The predicted DCX protein alteration is numbered with reference to the amino acid (aa) residue number. Amino acid substitution mutations are referenced by the wild-type amino acid and position followed by the mutant amino acid. For example, D9N indicates that the wild-type amino acid D at position 9 is mutated to an N. One or two base-pair deletions or insertions result in a translational reading frameshift followed by a protein termination codon. Mutations are indicated on the protein sequence of DCX that comprises two evolutionary conserved domains clustered in two repeats, namely, N-DC aa 46–139 and C-DC aa 173–263 depicted as pink boxes, and the N-terminal, the interdomain and the C-terminal linker are shown as light blue boxes. The mutations found in symptomatic females are indicated above the gene, and the deleted portions of the gene as thick lines and mutations found in asymptomatic females are shown in black boxes below the gene schema. An asterisk denotes the mutations described in this article. Severe forms with SBH grade 3–4 are denoted in red, and milder forms with SBH grade 1–2 are denoted in black. Inherited mutations are underlined.

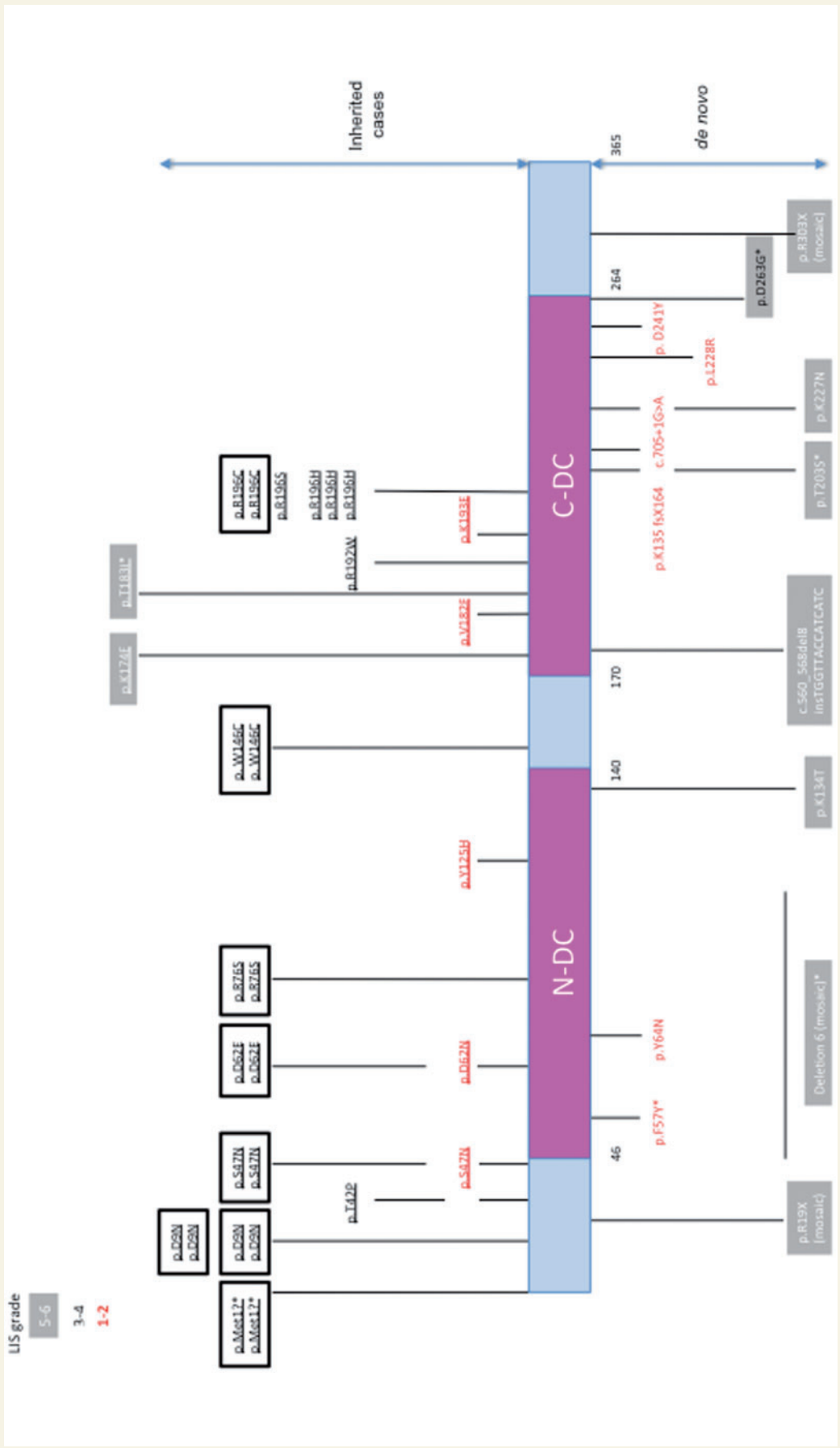

Figure 2 Schematic representation of the DCX protein and summary of the mutations identified in males with lissencephaly. Each *DCX* nucleotide mutation is numbered with reference to the ATG. The predicted DCX protein alteration is numbered with reference to the amino acid (aa) residue number. Mutations are indicated on the protein sequence of DCX that comprises two evolutionary conserved domains clustered in two repeats, namely, N-DC aa 46–139 and C-DC aa 173–263 depicted as pink boxes, and the N-terminal, the interdomain and the C-terminal linker are shown as light blue boxes. The inherited mutations are indicated above the gene, the families with two brothers affected are figures in black boxes, and *de novo* mutations found are shown below the gene scheme and the deleted portions of the gene as thick lines. An asterisk denotes the mutations described in this article. Severe forms with LIS grade 1–2 are denoted in red, intermediate forms with LIS grade 3–4 are denoted in black, and in light grey boxes are the milder forms with LIS grade 5–6. Inherited mutations are underlined.

Table 1 Overview of all *DCX* mutations in females with SBH

Patient number	Status	*De novo*/ inherited	Rapport XI	Nomenclature	Mutation type	Location	3D modelization and putative consequences on DCX function		Band
							NonInter/ destab	MT Y/N	
DCX_SBH_01	Propositus	*de novo*	N/A	c.55C > T p.R19X	Nonsense				Gr 2
DCX_SBH_02	Propositus	*de novo*	N/A	c.55C > T p.R19X	Nonsense				Gr 3
DCX_SBH_03	Propositus	*de novo*	55/45	**c. 91_92 insA p.H31Qfsx36**	Nonsense				Gr 2
DCX_SBH_04	Propositus	*de novo*	N/A	c.115C > T p.R39X	Nonsense				Gr 3
DCX_SBH_05	Propositus	*de novo*	60/40	c.115C > T p.R39X	Nonsense				Gr 4
DCX_SBH_06	Propositus	*de novo*	N/A	c.115C > T p.R39X	Nonsense				Gr 4
DCX_SBH_010	Propositus	*de novo*	75/25	c.505C > T p.Q169X	Nonsense				Gr 3
DCX_SBH_012	Propositus	*de novo*	N/A	**c.577A > T p.K193X**	Nonsense				Gr 4
DCX_SBH_016	Propositus	*de novo*	N/A	c.703C > T p.Q235X	Nonsense				Gr 3
DCX_SBH_019	Propositus	*de novo*	16/84	c.814C > T p.R272X	Nonsense				Gr 3
DCX_SBH_020/family_1	Propositus	Inherited	49/51	c.814C > T p.R272X	Nonsense				Gr 3
DCX_SBH_021/family_1	Female carrier	Inherited	80/20	c.814C > T p.R272X	Nonsense				Gr 2
DCX_SBH_022	Propositus	*de novo*	20/80	c.907C > T p.R303X	Nonsense				Gr 3
DCX_SBH_023	Propositus	*de novo*	70/30	c.947C > T p.R303X	Nonsense				Gr 3
DCX_SBH_024	Propositus	*de novo*	N/A	c.907C > T p.R303X	Nonsense				Gr 4
DCX_SBH_08	Propositus	*de novo*	59/41	**c.366-2A > C**	Splice				Gr 3
DCX_SBH_017	Propositus	*de novo*	62/38	c.705 + 1G > A	Splice				Gr 4
DCX_SBH_018	Propositus	*de novo*	N/A	**c.828 + 1G > A**	Splice				Gr 4
DCX_SBH_07	Propositus	*de novo*	50/50	**c.285_286delA p.N96TfsX55**	Frameshift				Gr 3
DCX_SBH_09	Propositus	*de novo*	N/A	**c.442_443delG p.V148FfsX3**	Frameshift				Gr 4
DCX_SBH_011	Propositus	*de novo*	76/24	**c.528_529insT**	Frameshift				Gr 4
DCX_SBH_013	Propositus	*de novo*	52/48	**c.579_580delG p.A194LfsX5**	Frameshift				Gr 4
DCX_SBH_014	Propositus	*de novo*	100/0	**c.681_682insA**	Frameshift				N/A
DCX_SBH_015	Propositus	*de novo*	57/43	**c.682_683delCT p.L228LfsX13**	Frameshift				Gr 2
DCX_SBH_087	Propositus	*de novo*	N/A	c.1078delG	Frameshift				Gr 2
DCX_SBH_026/family_3	Female carrier	Inherited	N/A	c.25G < A p.D9N	Missense	N terminal linker			Absent
DCX_SBH_027/family_4	Female carrier	Inherited	100/0	c.25G < A p.D9N	Missense	N terminal linker			Absent
DCX_SBH_028/family_5	Female carrier	Inherited	56/44	c.124 A > C p.T42P	Missense	N terminal linker			Absent
DCX_SBH_029	Propositus	*de novo*	55/45	**c.94G > C p.A33P**	Missense	N terminal linker			Gr 4
DCX_SBH_030/family_6	Female carrier	Inherited	N/A	c.140G > A p.S47N	Missense	N terminal linker	NI	MT Y	Gr 2
DCX_SBH_031/family_7	Female carrier	Inherited	100/0%	c.140G > Ap.S47N	Missense	N terminal linker	NI	MT Y	Absent
DCX_SBH_032	Propositus	*de novo*	47/53	c.176G > A p.R59H	Missense	N-DC surface	HD	Possible MT binding	Gr 3
DCX_SBH_033	Propositus	*de novo*	46/54	c.176G > A p.R59H	Missense	N-DC surface	HD	Possible MT binding	Gr 3
DCX_SBH_036	Propositus	*de novo*	31/69	c.227G > C p.R76P	Missense	N-DC surface	LD	MT Y	Gr 3

(continued)

Table 1 Continued

Patient number	Status	*De novo*/ inherited	Rapport XI	Nomenclature	Mutation type	Location	3D modelization and putative consequences on DCX function		Band
							NonInter/ destab	MT Y/N	
DCX_SBH_037/family_10	Female carrier	Inherited	N/A	c.226C > A p.R76S	Missense	N-DC surface	NI	MT Y	Absent
DCX_SBH_038	Propositus	*de novo*	N/A	c.232C > T p.R78C	Missense	N-DC surface	NI	MT Y	Gr 4
DCX_SBH_039	Propositus	*de novo*	36/64	c.233G > A p.R78H	Missense	N-DC surface	NI	MT Y	Gr 2
DCX_SBH_040	Propositus	*de novo*	52/48	c.233G > T p.R78L	Missense	N-DC surface	NI	MT Y	Gr 4
DCX_SBH_041	Propositus	*de novo*	80/20	**c.263C ⩾ A p.T88K**	Missense	N-DC surface	LD	MT Y	N/A
DCX_SBH_043	Propositus	*de novo*	60/40	**c.304C ⩾ T p.R102C**	Missense	N-DC surface	NI	MT Y	Gr 2
DCX_SBH_045	Propositus	*de novo*	61/39	c.364G > T p.G122W	Missense	N-DC surface	HD	MT N	Gr 4
DCX_SBH_049	Propositus	*de novo*	N/A	c.386C ⩾ T p.S129L*	Missense	N-DC surface	LD	Possible MT binding	Gr 3
DCX_SBH_050	Propositus	*de novo*	67/33	**c.400A ⩾ G p.K134E**	Missense	N-DC surface	NI	Possible MT binding	Gr 2
DCX_SBH_034/family_8	Female carrier	Inherited	N/A	c.186C > G p.D62E	Missense	N-DC buried	HD	MT N	Gr 1
DCX_SBH_035/family_9[a,b]	Female carrier	Inherited	N/A	c.184G > A p.D62N	Missense	N-DC buried	LD	MT N	Gr 2
DCX_SBH_042	Propositus	*de novo*	53/47	**c.301G > C p.V101L**	Missense	N-DC buried	LD	MT N	Gr 4
DCX_SBH_044	Propositus	*de novo*	60/40	**c.356T > C p.L119P**	Missense	N-DC buried	HD	MT N	Gr 3
DCX_SBH_046[b]	Propositus	*de novo*	N/A	c.373T > G p.Y125D	Missense	N-DC buried	HD	MT N	Gr 4
DCX_SBH_047 Family_11[a,b]	Daughter	Inherited	N/A	c.373T > C p.Y125H	Missense	N-DC buried	HD	MT N	Gr 3
DCX_SBH_048 Family_11[a,b]	Female carrier	Inherited	N/A	c.373T > C p.Y125H	Missense	N-DC buried	HD	MT N	Gr 2
DCX_SBH_051/family_12	Female carrier	Inherited	25/75	c.520A > G p.K174E	Missense	N-DC_C-DClinker	NI	Possible MT binding	Absent
DCX_SBH_052	Propositus	*de novo*	59/41	**c.529T > G p.V177G**	Missense	N-DC_C-DClinker	LD	Possible MT binding	Gr 4
DCX_SBH_053	Propositus	*de novo*	44/56	c.536C > T p.P179L	Missense	C-DC surface	LD	Possible MT binding	Gr 4
DCX_SBH_055/family_14	Female carrier	Inherited	75/25	**c.548C > T p.T183I***	Missense	C-DC surface	LD	MT N	Absent
DCX_SBH_056	Propositus	*de novo*	N/A	c.556 C > T p.R186C*	Missense	C-DC surface	HD	Possible MT binding	Gr 4
DCX_SBH_057	Propositus	*de novo*	N/A	c.556C > T p.R186C*	Missense	C-DC surface	HD	Possible MT binding	Gr 4
DCX_SBH_058	Propositus	*de novo*	25/75	c.556C > T p.R186C*	Missense	C-DC surface	HD	Possible MT binding	Gr 4
DCX_SBH_059	Propositus	*de novo*	63/37	c.556C > T p.R186C*	Missense	C-DC surface	HD	Possible MT binding	Gr 4
DCX_SBH_060	Propositus	*de novo*	N/A	c.556C > T p.R186C*	Missense	C-DC surface	HD	Possible MT binding	Gr 4
DCX_SBH_061	Propositus	*de novo*	80/20	c.556C > T p.R186C*	Missense	C-DC surface	HD	Possible MT binding	Gr 4
DCX_SBH_062	Propositus	*de novo*	43/57	c.557G > T p.R186H*	Missense	C-DC surface	HD	Possible MT binding	Gr 4
DCX_SBH_063	Propositus	*de novo*	67/33	c.557G > T p.R186H*	Missense	C-DC surface	HD	Possible MT binding	Gr 4
DCX_SBH_064	Propositus	*de novo*	31/69	c.557G > T p.R186H*	Missense	C-DC surface	HD	Possible MT binding	Gr 3
DCX_SBH_065	Propositus	*de novo*	75/25	c.557G > T p.R186H*	Missense	C-DC surface	HD	Possible MT binding	Gr 2
DCX_SBH_066	Propositus	*de novo*	44/56	c.557G > T p.R186H*	Missense	C-DC surface	HD	Possible MT binding	Gr 4
DCX_SBH_067	Propositus	*de novo*	100/0	c.557G > A p.R186H*	Missense	C-DC surface	HD	Possible MT binding	Gr 3
DCX_SBH_068	Propositus	*de novo*	N/A	c.557G > T p.R186L*	Missense	C-DC surface	HD	Possible MT binding	Gr 4
DCX_SBH_069/family_15[a,b]	Female carrier	Inherited	100/0	c.574C > Tp.R192W	Missense	C-DC surface	HD	Possible MT binding	Gr 1

(continued)

Table 1 Continued

Patient number	Status	*De novo*/ inherited	Rapport XI	Nomenclature	Mutation type	Location	3D modelization and putative consequences on DCX function		Band
							NonInter/ destab	MT Y/N	
DCX_SBH_070/family_15[a,b]	Daughter	Inherited	N/A	c.574C > Tp.R192W	Missense	C-DC surface	HD	Possible MT binding	Gr 2
DCX_SBH_071/family_15[a,b]	Daughter	Inherited	N/A	c.574C > Tp.R192W	Missense	C-DC surface	HD	Possible MT binding	Gr 2
DCX_SBH_072	Propositus	*de novo*	44/56	c.574C > T p.R192W	Missense	C-DC surface	HD	Possible MT binding	Gr 2
DCX_SBH_073	Propositus	*de novo*	60/40	c.574C > T p.R192W	Missense	C-DC surface	HD	Possible MT binding	Gr 3
DCX_SBH_074/family_16	Female carrier	Inherited	N/A	c. 576 A > G p.K193E*	Missense	C-DC surface	NI	MT N	Absent
DCX_SBH_075/ Family_17	Female carrier	Inherited	53/47	c.586C > T p.R196C	Missense	C-DC surface	NI	Possible MT binding	Absent
DCX_SBH_076/family_18	Female carrier	Inherited	23/77	c.586C > T p.R196C	Missense	C-DC surface	NI	Possible MT binding	Absent
DCX_SBH_077/family_19	Female carrier	Inherited	N/A	c.586C > A p.R196S	Missense	C-DC surface	NI	Possible MT binding	Gr 1
DCX_SBH_078/family_20	Female carrier	Inherited	N/A	c.587G > A p. R196H	Missense	C-DC surface	NI	Possible MT binding	Absent
DCX_SBH_079/family_21	Female carrier	Inherited	80/20	c.587G > A p. R196H	Missense	C-DC surface	NI	Possible MT binding	Absent
DCX_SBH_080/family_22	Female carrier	Inherited	N/A	c.587G > A p. R196H	Missense	C-DC surface	NI	Possible MT binding	Gr 1
DCX_SBH_081	Propositus	*de novo*	47/53	**c.593T > C p.L198P**	Missense	C-DC surface	LD	Possible MT binding	Gr 4
DCX_SBH_085	Propositus	*de novo*	51/49	c.728T > C p.F243S	Missense	C-DC surface	NI	Mt N	Gr 2
DCX_SBH_083[b]	Propositus	*de novo*	N/A	c.668G > A p.G223E	Missense	C-DC surface	HD	Possible MT binding	Gr 3
DCX_SBH_054/family_13	Female carrier	Inherited	51/49	c.544g > t p.V182F	Missense	C-DC buried	HD	MT N	Gr1
DCX_SBH_082[b]	Propositus	*de novo*	N/A	c.640T > C p.I214T	Missense	C-DC buried	HD	MT N	Gr 2
DCX_SBH_084	Propositus	*de novo*	63/37	**c.707T > A p.V236E**	Missense	C-DC buried	HD	MT N	Gr 3
DCX_SBH_086[b]	Propositus	*de novo*	N/A	c.769T > C p.I250T	Missense	C-DC buried	LD/HD ?	MT N	Gr 3
DCX_SBH_089/family_25	Daughter	Inherited	70/30	**Dup Exon 4-7**	Duplication				Gr 4
DCX_SBH_090/family_25	Daughter	Inherited	63/37	**Dup Exon 4-7**	Duplication				Gr 4
DCX_SBH_091/family_25	Female carrier	Inherited	47/53	**Dup Exon 4-7**	Duplication				Absent
DCX_SBH_092/family_25	Female carrier	Inherited	60/40	**Dup Exon 4-7**	Duplication				Absent
DCX_SBH_093	Propositus	*de novo*	100/0	**Del exon 1-2**	Deletion				Gr 4
DCX_SBH_025/family_2	Female carrier	Inherited	100/0	**c.2T > A p.Met1?**	Unclassified				Gr 1
DCX_SBH_088/family_23	Female carrier	Inherited	N/A	**(c.1144 T > A) X361Phe48X**	Unclassified				Gr 1

Mutations in bold are newly described here.
Possible MT binding indicates residues on the surface of C-DC that, based on modelling, may interact with microtubules, but the partners and role of this subdomain are still poorly understood.
Surface mutations with partially buried side chains are marked with an asterisk. Further structural information is available on request.
a Patients previously reported in des Portes *et al*. (1998*a*).
b Patients previously reported in des Portes *et al*., (1998*b*).
Gr = grade; XI = X inactivation; N/A = not available; NI = non-internal residues, which are non-destabilizing; HD = highly destabilizing; LD = less destabilizing; microtubule MT Y/N = interacts with microtubules (Y) or not (N).

Table 2 Overview of neurological data in 14 male patients with intragenic *de novo* mutations in the *DCX* gene

	Reference	Group	Mutation type	Location	3D modelization and putative consequenceson DCX function		LIS grade	Age (yrs)*	Motor development	Epilepsy	
					Non Inter/ destab	MT Y/N				Age of onset (yrs)	Sz control
XLIS_36[a]	DCX_006	Nonsense (mosaic)	c.55C > T p.R19X				6	28	Normal	6	Refractory
XLIS_37[a]	DCX_029	Nonsense (mosaic)	c.947C > T p.R303X				6	12	Normal	17	Partially controlled
XLIS_30	This series	Splice	c.705 +1 G > A				1		Spastic tetraplegia	0,3	Refractory
XLIS_26[a]	DCX_030	Frameshift	c.403_404delAA p.K135fsX164				1	3	Tetraplegia	0.3	Refractory
XLIS_38[a]	DCX_019	Frameshift	c.560_568del8insTGGTTACCATCATC				6	34	Normal	N/A	N/A
XLIS_03[a]	DCX_026	Missense	c.190T > A p.Y64N	N-DC surface	NI	MT Y	2	24	Spastic tetraplegia	0.1	Refractory
XLIS_40	This series	Missense	**c.401A > C p.K134T**	**N-DC surface**	NI	**Possible MT binding**	5	3	Tetraplegia	0.5	Refractory
XLIS_09	This series	Missense	**c.170 T > A p.F57Y**	**N-DC buried**	LD	MT N	1	2	Spastic tetraplegia	0.1	Refractory
XLIS_22[a]	DCX_025	Missense	c.607A > T p.T203S	C-DC surface	LD	**Possible MT binding**	5	5	Normal	0.2	Refractory
XLIS_29[a]	DCX_015	Missense	c.681A > T p.K227N	C-DC surface	NI	**Possible MT binding**	5	7	Normal	2	Controlled
XLIS_23[a]	DCX_024	Missense	c.741G > T p.D241Y	C-DC surface	LD	MT N	1	4	Tetraplegia	0.2	Refractory
XLIS_27	This series	Missense	c. 788 A > G p.**D263G**	C-DC surface	LD	MT N	3	17	Normal	17	Controlled
XLIS_28[a]	DCX_021	Missense	c. 683 T > G p. L228R	C-DC buried	HD	MT N	2	3	Tetraplegia	0.5	Refractory
XLIS39	This series	Deletion (mosaic)	Deletion Exon 6				6	4	Tetraplegia	0.3	Refractory

LIS grade (Dobyns *et al*., 1999). Age refers to age at last evaluation. Possible MT binding indicates residues on the surface of C-DC that, based on modelling, may interact with microtubules, but the partners and role of this subdomain are still poorly understood. Further structural information is available on request.

a Males previously reported in Leger *et al*. (2008).

Yrs = years; sz = seizure; N/A = not available; Bold = newly described mutations; NI = non-internal residues, which are non-destabilizing; HD = highly destabilizing; LD = less destabilizing; MT Y/N = interacts with microtubules (Y) or not (N).

carriers and six daughters) (Supplementary Tables 1 and 2). Of note, the symptomatic carriers showed minor neurological signs in all cases and were diagnosed with SBH during pregnancy ($n = 3$) or when their son(s) were diagnosed with lissencephaly. Fourteen other mothers with *DCX* mutations were asymptomatic, that is, no history of epilepsy, normal neurological development and normal MRI ($n = 13$) and one carrier female for whom no data were available.

In female patients with SBH, presenting symptoms were epileptic seizures (47%), including infantile spasms or developmental delay (16.6%). At last evaluation, all patients with SBH except two had intellectual disability assessed to be moderate to severe. Impairments included abnormal language development and use (67.1%) and moderate to severe behavioural disturbances (59.7%). The latter mainly consisted of hyperkinetic movements, crying and automutilation, and occasionally, autistic features with perseveration, echolalic language and stereotypical behaviour. A significant proportion of patients displayed an abnormal neurological examination, usually truncal hypotonia or spasticity (29%) and microcephaly (15.6%). Seizure disorders were present in 84.9% patients, where seizures started mainly in infancy (34.5%) or during childhood (45%). At onset and at last evaluation, most cases with SBH had either polymorphic seizures with a combination of atonic and tonic seizures, atypical absences and/or epileptic spasms or focal seizures. Classifying these patients by epileptic syndrome, we identified 31 patients presenting with Lennox–Gastaut syndrome, 10 with focal epilepsy, and 17 with generalized epilepsy. Seizure control is highly variable, with a high proportion of drug resistance (78.3%) (Supplementary Tables 1 and 2).

Brain MRI was performed in all patients (summarized in Table 1 and Supplementary Table 2) at a mean age of 14.5 years (median: 8 years, ranging from 6 months to 60 years). Brain MRI revealed two major groups. First was the most severe form with a thick (>8 mm) continuous band around the entire brain (SBH grade 3–4) (Fig. 3) ($n = 42$). Close to this SBH pattern is a pattern suggestive of lissencephaly on T_1-weighted images with increased cortical thickness and poor differentiation of the cortex and underlying white matter and thick heterotopic bands on T_2-weighted images (Fig. 4); this latter pattern was identified in 12 children aged <2 years for whom MRI data were already available because of early-onset epilepsy. A second milder form with a thin band (SBH grade 1–2; 4–7 mm) was identified either only present in the frontal lobe or restricted to the frontal and temporal lobes with intermediate thickness. This pattern was observed either in symptomatic female carriers (13/25; 52%) or sporadic patients (11/61; 18%).

Brain abnormalities observed in SBH are mostly prominent in cortical structures. Considering the corpus callosum abnormalities that were identified, these included a dysmorphic ($n = 24$) or thin corpus callosum ($n = 6$), and one case of posterior corpus callosum agenesis. No significant white matter abnormalities were noted. Cerebellar abnormalities are also variable and comprised mild vermian hypoplasia in three cases. Dilatation of the fourth ventricles without pontocerebellar abnormalities was noted in 14 cases. Finally, the occurrence of microcephaly was 15.6%.

Quantitative volumetric analysis of the cortex and the heterotopic bands was performed in eight patients for whom the resolution of the images and 3D T_1-weighted sequences were available (Supplementary Fig. 2). Although data are preliminary due to the small number of cases analysed, the ratio of the subcortical band volumes in patients with SBH grade 1–2 ranged from 5.67 to 9.26% of the total grey matter volume, while in those with more severe SBH grade 3–4, the ratio ranged from 12.21 to 27.2%, confirming the 2D evaluation of the thickness of the band.

To determine whether MRI can contribute to the prediction of the history and clinical outcome of patients with SBH, we compared the severity of intellectual disability, behavioural disturbances and epilepsy with band thickness and the degree of cortical abnormalities (Table 3). Two groups could be defined according to band thickness. Patients with diffuse thick bands with anterior predominance ($n = 54$) showed significantly more shallow or very shallow sulci in frontal regions ($P < 0.001$), moderate to severe ventricular enlargement ($P < 0.001$) and prominent perivascular spaces in subcortical or periventricular regions or both ($P < 0.001$). Clinical presentation is also determined by band thickness, with a higher proportion of epileptic encephalopathy at onset (68.6%) or developmental delay (31.4%) ($P < 0.001$) in patients with a thicker band. At last evaluation, most patients with a thicker band were severely intellectually impaired ($P < 0.001$), with only two patients having age-appropriate language, while most had either no words or poor verbal skills (84%) ($P < 0.001$). Moreover, they showed a higher proportion of severe behavioural disturbances (77.8%) ($P < 0.001$). At the other end of the spectrum, patients with thin SBH (15.2%) displayed a normal cortical aspect or slightly shallow sulci, with no ventriculomegaly. None demonstrated intellectual disability or severe behavioural disturbances. Seizure occurrence was not determined by band thickness since most patients with thicker bands (82%) show epilepsy of the Lennox–Gastaut syndrome type (55.3%). Similarly, 91.3% of patients with thin bands have epilepsy, with a large proportion of Lennox–Gastaut syndrome (50%). However, most patients with thicker bands started experiencing seizures early in infancy (with a median age of onset of 2.2 years) compared with those with a thinner band (median age of seizure onset: 10 years, $P = 0.0002$). Female carriers with normal MRI ($n = 14$) without a visible band were clinically normal and demonstrated neither neurological symptoms nor epileptic seizures. These data outline the importance of band thickness in the determination of the neurological prognosis of patients with SBH.

Clinical and radiological presentations of male patients with DCX mutations

Our previous data suggested that sporadic males with *de novo* *DCX* mutations have a more severe presentation, but the trend did not reach statistical significance. To improve statistical power, we added four new males with inherited mutations and five with *de novo* mutations to the patients described in the previous study (Leger *et al.*, 2008). Altogether, 43 male patients with lissencephaly were evaluated, including 29 with inherited mutations and 14 with *de novo* mutations (see Table 2 and Supplementary

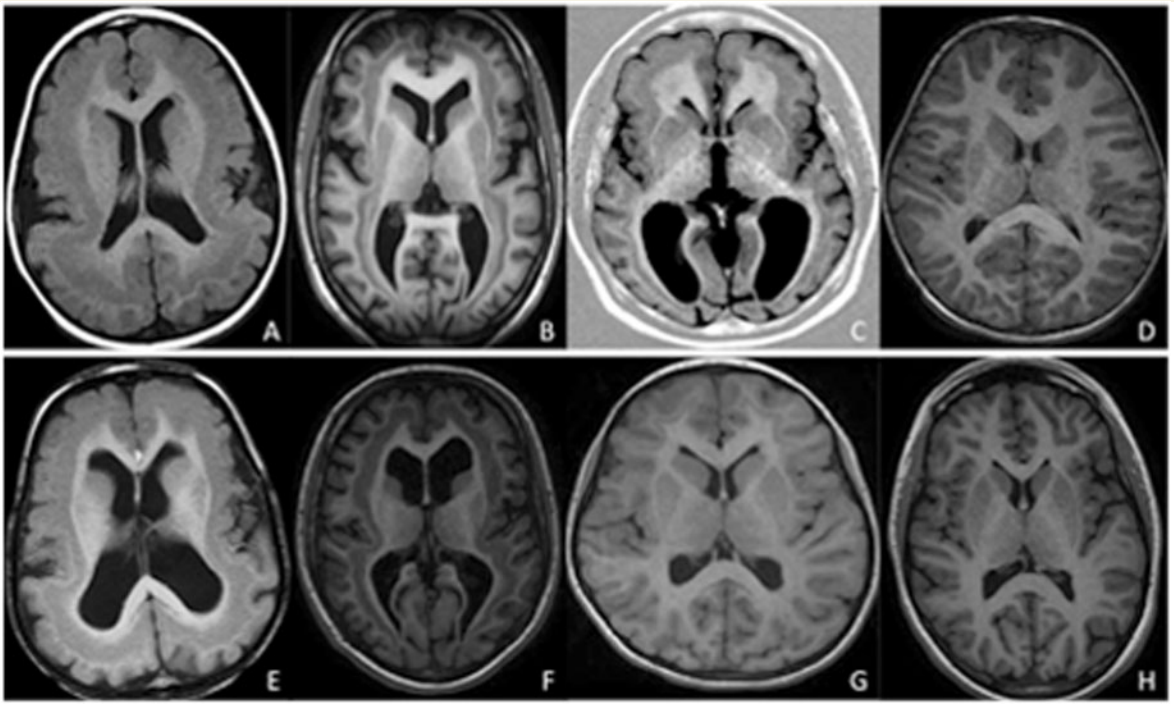

Figure 3 Variable extent and thickness of band in cases with sporadic SBH. Representative MRI scans in patients with either a thick continuous band around the entire brain (grade 3–4) (**A**, **B**, **E** and **F**) or a thinner band only present in the frontal lobe (**G**) or restricted to the frontal and temporal lobe with intermediate thickness (grade 2) (**C**). Thick and continuous band around the entire brain in two patients aged 2 years and 11 months (**A**) and 3 years and 6 months (**E**), respectively. The bands appear to fuse with the outer cortex in the frontal regions. Intermediate diffuse SBH in two patients aged 15 (**B**) and 16 years (**F**). Thin band only present in the frontal lobe (**G**) or restricted to the frontal and the temporal lobe (**C**) in two patients aged 24 years and 11 years. **D** and **H** are from control patients aged 3 and 15 years, respectively.

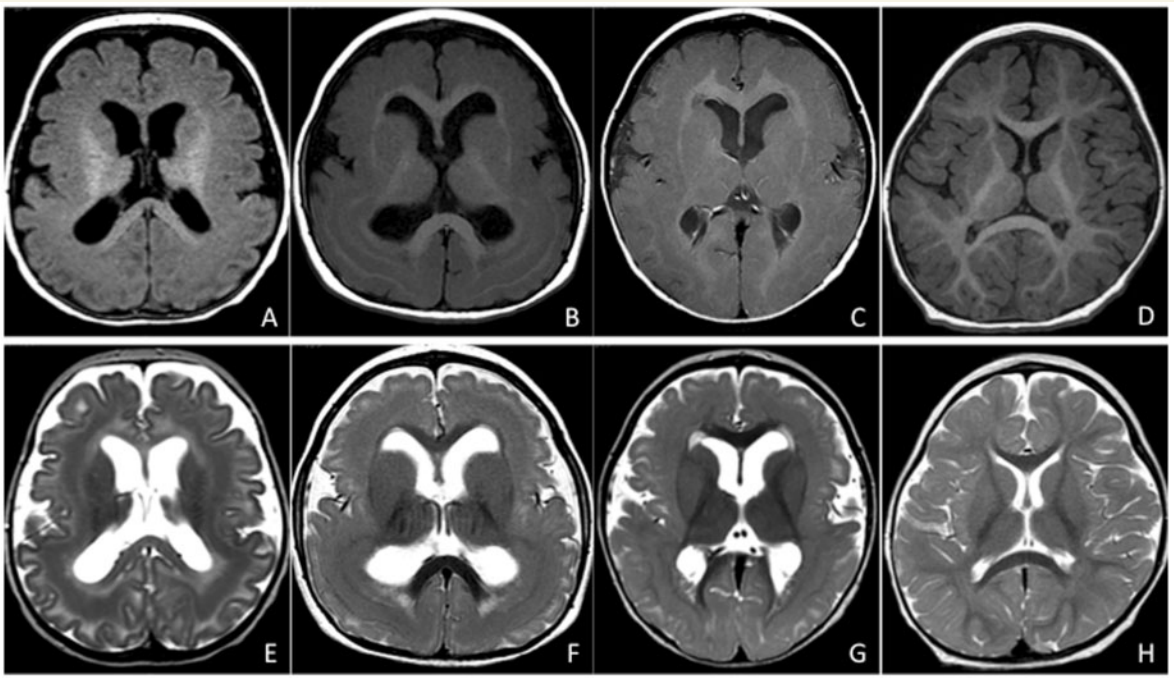

Figure 4 Representative axial MRI in young children aged 7 months (**A** and **E**), 14 months (**B** and **F**) and 17 months (**C** and **G**). T_1-weighted images show poor differentiation of the cortex and underlying white matter, with an aspect reminiscent of diffuse pachygyria (in younger child, **A**), or frontoparietal pachygyria combined with band heterotopia in posterior regions (in patients >1 year of age, **B** and **C**). At the same level, on T_2-weighted images, the band is visible (**E**, **F** and **G**). Control MRI: T_1-weighted image (**D**) and T_2-weighted image (**H**) in a normal 15-month-old female.

Table 3 Comparison of female cases with SBH and *DCX* mutations according to severity

	Severe (SBH Gr3-4)[a]	Intermediate (SBH Gr1-2)[a]	Absent SBH	*P*-value
Total	54	24	14	
Age at last evaluation (median [range])	10 years [1–45]	25 years [5.4–44]	37 years [10–65]	
Status				<0.001
Inherited mutations (*n* = 31) (25 females carriers)	3 mutations (4 patients)	11 mutations (13 patients)	11 mutations (14 patients)	
***De novo* mutations (*n* = 61)**	36 mutations (50 patients	11 mutations (11 patients)	0	
DCX mutation type				
Nonsense and deletion (*n* = 18[b])	14 mutations (20 patients)	5 mutations (5 patients)	1 mutation (2 patients)	
Missense N-DC (*n* = 17[c])	11 mutations (10 patients)	6 mutations (6 patients)	1 mutation (1 patient)	
Missense C-DC (*n* = 17[d])	9 mutations (18 patients)	7 mutations (10 patients)	4 mutations (6 patients)	
Missense N terminal domain–interdomain (*n* = 6[e])/splicing defect (*n* = 3)	5 mutations (5 patient)	1 mutation (1 patient)	4 mutations (5 patients)	
Unclassified (*n* = 2)	0	2 mutations (2 patient)	0	
Skewed inactivation (%)	6/36 (16.7)	3/12 (25)	3/7 (42.9)	0.29
Moderate to severe ventriculomegaly (*n* = 88) (%)	37/53 (69.8)	2/21 (9.5)	0/14 (0)	0.001
Prominent perivascular spaces (*n* = 77) (%)	33/45 (73.3)	7/19 (36.8)	0/13 (0)	0.001
Presenting symptoms				0.001
Mother carrier (%)	0/51 (0)	9/23 (39.1)	14/14 (100)	
Developmental delay (%)	16/51 (31.4)	1/23 (4.3)	0/14 (0)	
Seizures (including West) (%)	35/51 (68.6)	13/23 (56.5)	0/14 (0)	
Microcephaly (*n* = 68) (%)	7/45 (15.6)	0/18 (0)	0/5 (0)	0.24
Moderate to severe ID (*n* = 86) (%)	47/51 (92.2)	9/21 (42.9)	0/14 (0)	0.001
Severe language delay i.e. absent word or poor verbal skills (*n* = 87) (%)	42/50 (84)	7/23 (30.4)	0/14 (0)	<0.001
Moderate to severe behavioural disturbances (*n* = 81) (%)	35/45 (77.8)	5/22 (22.7)	0/14 (0)	<0.001
Patients who developed epilepsy (*n* = 87) (%)	41/50 (82)	21/23 (91.3)	0/14 (0)	<0.001
Early-onset seizures < 1 year (*n* = 55) (%)	18/38 (47.4)	1/17 (5.9)		0.003
Seizure type at last evaluation (*n* = 58)				0.16
Lennox–Gastaut type[f] (%)	21/38 (55.3)	10/20 (50)		
Focal seizures (including with secondary generalization) (%)	4/38 (10.5)	6/20 (30)		
Intractable epilepsy (*n* = 60) (%)	34/40 (85)	13/20 (65)		0.1

a The number of the denominator indicates the number of patients in whom specific information was available.
b R272X was identified in severe and intermediate SBH and duplication of exon 4-7 was found in one family with both severe SBH and absent SBH.
c Y125H was found in one family with the female carrier with grade 1–2 and her daughter with grade 4.
d Three mutations were found in different groups: R192W found in the same family with grade 1 in all females, and in two cases with *de novo* mutations with grade 2 and grade 3 SBH, respectively. R186H was found in five cases with grade 3–4 SBH and in one case with SBH grade 2 (intermediate). Also, the recurrent mutation R196H was found in the two groups with absent and intermediate SBH.
e S47N was found in an asymptomatic female carrier (absent SBH) and one symptomatic female carrier.
f Includes polymorphic seizures, i.e. generalized tonic seizures, atypical absences and drop attacks.
N/A = not available; ID = intellectual disability.

Table 2). We now confirm that male patients with *de novo DCX* mutations tend to have more severe neurological presentation, including a higher proportion of seizures at onset and more frequently diffuse agyria. *De novo* mosaic mutations (3/14) gave a milder phenotype with anterior pachygyria and SBH (LIS grade 6) (Dobyns and Truwit, 1995). Cases with lissencephaly with inherited mutations showed a more homogeneous phenotype with anterior agyria or pachygyria (LIS grade 3–4 86.4%) (Fig. 5) and developmental delay at onset (Table 4). Interestingly, similarly to females with either thin or thick SBH, no differences in seizure occurrence and response to antiepileptic drugs were found between the groups, suggesting that the epileptogenicity is not strictly related to the degree of agyria–pachygyria.

Genotype–phenotype correlations

To gain further insight into the relationship between mutation type and phenotype, we compared the characteristics of *DCX* mutations among the cohort of patients with SBH (Tables 1 and 3).

Firstly, it is noteworthy that the most severe group (SBH grade 3–4) shows a large proportion of *de novo* mutations, while only four patients had inherited mutations. In this group in which 38 different mutations were identified, one-third of mutations were nonsense, frameshift or deletion, while the remaining were missense. In contrast, approximately half of the milder forms (SBH grade 1–2) were due to inherited mutations (54.2%), the majority found in symptomatic female carriers.

Secondly, none of the *de novo* SBH *DCX* mutations were responsible for LIS in sporadic males, except one splice mutation (c.705 + 1G > A), suggesting that the severity and the impact of these mutations on *DCX* are different. Nonsense mutations were never associated with lissencephaly, except mosaic cases not included in our statistical analyses. No major overall differences were found in the distribution of the mutations according to their location in either N-DC or C-DC, representing 25.3 and 30.3% of *DCX* mutations, respectively. This represents 28.9 versus 24.4% in *de novo* mutations in females, 21.1 versus 35.7% in *de novo* mutations in males, and 20 versus 40% in *de novo* mutations in inherited cases. Of note, the higher percentage of inherited cases with C-DC mutations increases further if recurrent mutations are included. Thus, C-DC mutations, in general, appear quite prominent.

We next examined patients with SBH and recurring missense mutations at either Arg186, Arg196, or Arg78. We observed that these mutations are associated with distinct phenotypes. The mutation Arg196 located on the surface of C-DC (Table 1) was carried only in inherited case**s** ($n = 6$; Supplementary Table 2). Moreover, the phenotype was milder in both genders, with females demonstrating either normal MRI and clinical presentation (4/6) or thin SBH (2/6) with minor epilepsy. Affected boys showed anterior pachygyria (LIS grade 4), ability to walk and partial to complete seizure control. Conversely, three recurrent mutations Arg186, Arg78 and Arg303 were found exclusively in patients with SBH with *de novo* mutations. Arg186 mutations ($n = 13$) leading to three different substituted residues (p.R186C, p.R186H and p.R186L) were clearly associated with a severe phenotype, with thicker SBH (92.3%) and severe intellectual disability (83.3%), whatever the substituted residue. Because no skewed inactivation was observed in lymphocyte DNA, this phenotype is probably directly related to the importance of this residue for C-DC stability. Other recurrent mutations on Arg303 ($n = 3$) and Arg78 ($n = 3$) were associated with heterogeneous clinical and radiological presentations. In the case of Arg303X, the different presentations may be related to skewed inactivation. Arg78 is a surface residue and predicted to directly participate in microtubule binding, phenotypic variability is likely therefore to be explained by the different amino acid substitutions leading to variable alterations of N-DC function. Thus, both the affected residue and the substituted amino acid determine the severity of the phenotype, with some mutations probably enabling more residual protein function than others.

We performed a finer analysis of predicted effects of missense mutations on N- or C-DC structure and function (Fig. 6 and Table 1), taking into account local or global destabilization of the domains. In males, we found that most of the missense mutations in N- and C-DC leading to severe phenotypes are destabilizing (6/8). Highly destabilizing mutations affect buried residues (p.Y125H, p.L228R and p.V182F); less destabilizing mutations affect either buried residues (p.D62N and p.F57Y) or surface residues where mutation is likely to influence the structure of the loop they are found in (p.D241Y). In addition, one further surface mutation is predicted to affect local interactions with microtubules (p.Y64N), and one final mutation leading to a severe phenotype in males (p.K193E) is on the surface but faces away from the microtubule interface, and may affect interactions with other binding partners. In females, severe phenotype missense mutations are also mainly destabilizing (p.R59H, p.R76P, p.V101L, p.L119P, p.G122W, p.Y125D/H, p.S129L, p.V177G, p.P179L, p.R186C/H/L, p.R192W, p.L198P, p.G223E, p.V236E and p.I250T). Of these, four are predicted to be less destabilizing, but also to perturb the interaction with microtubules (p.R76P, p.V177G, p.P179L and p.L198P). One further mutated residue is unlikely to be destabilizing, but is predicted to perturb the interaction with microtubules (p.R78C/L). Two further apparently less destabilizing mutations that produce severe phenotypes are either unlikely to be at the microtubule interface (p.V101L), or the interaction with microtubules is less certain (p.S129L). Thus, the majority of severe female missense mutations in N- and C-DC either destabilize the domain or affect interactions with microtubules. Interestingly, Arg59 in N-DC aligns with Arg186 in C-DC; both are destabilizing and give rise to severe phenotypes. These residues are conserved between the domains because they are most likely important for folding of the DC domain. Of note, highly destabilizing mutations in general give more severe phenotypes.

Moderate phenotypes in males are associated with either destabilizing effects (p.D62E, p.R192W and p.D263G) or surface residues likely to interact with (p.S47N and p.R76S), or possibly interacting with (p.R196C/H), microtubules. It is possible that mutations of these latter residues only affect affinity but still allow microtubule binding, which might explain the less severe phenotype. S47 is subject to phosphoregulation (Schaar *et al*., 2004), but the p.S47N mutation also gives only a mild phenotype in a female showing non-biased X-inactivation. p.D62E and p.R192W are predicted to be highly destabilizing, and the explanation for a

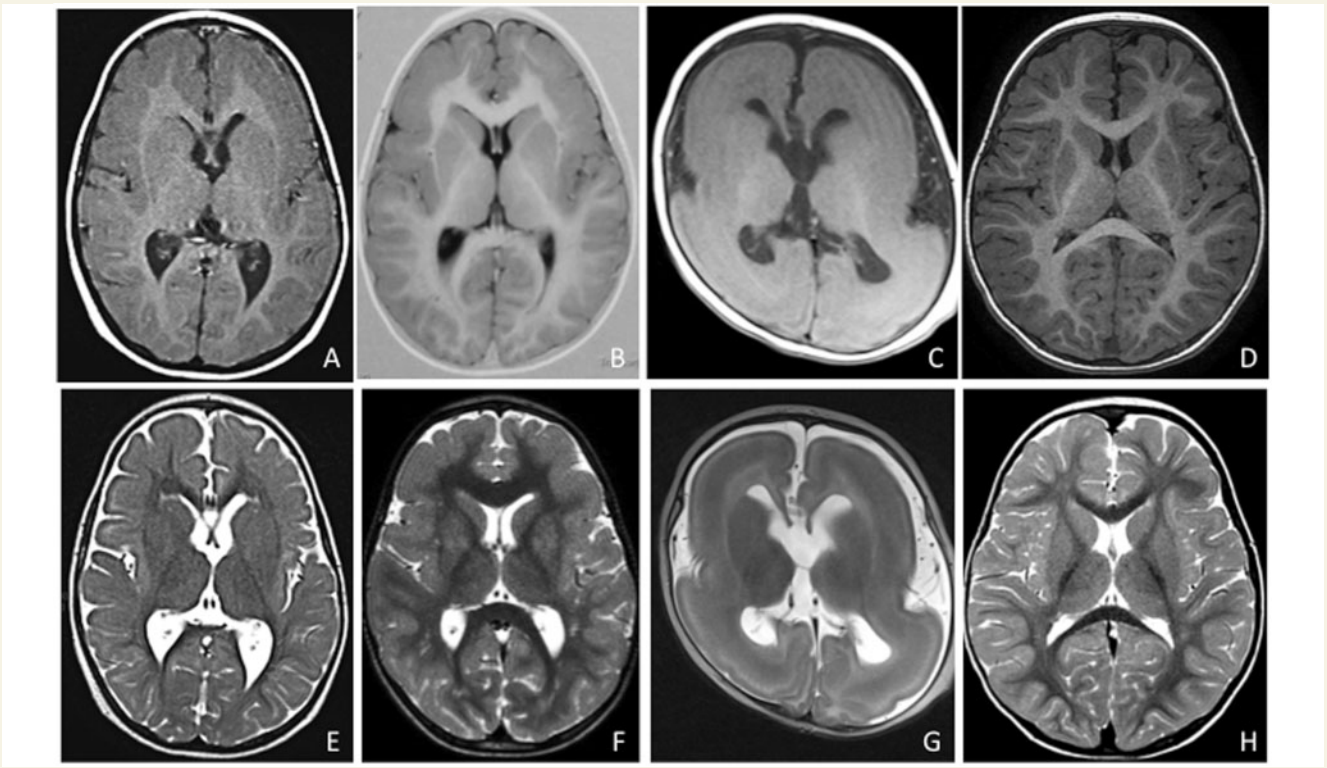

Figure 5 Representative T_1-weighted (**A**, **B** and **C**) and T_2-weighted (**E**, **F** and **G**) axial section of MRI in three males with *DCX* mutations representing the most prominent LIS grade in this study. Anterior pachygyria (LIS grade 4) in a 2-year-old male (familial case) (**A** and **E**). SBH with anterior pachygyria in a 5-year-old male (familial case) (**B** and **F**). Severe lissencephaly (LIS grade 2) more severe anteriorly in a sporadic male aged 1 year 3 months (**C** and **G**). Control MRI: T_1-weighted image (**D**) and T_2-weighted image (**H**) in normal 18-month-old boy.

moderate and not severe phenotype is therefore not obvious. Undetected mosaicism may be one possible explanation. Of the mild phenotypes in males, one is a surface mutation not predicted to interact with microtubules (p.K227N), two further are surface mutations where interactions with microtubules are possible but not certain (p.K134T and p.T203S), one is a residue in the inter-domain linker (p.K174E), which might, however, also interact with microtubules, and finally, one mutation of a surface residue with a partially buried side chain (p.T183I) may be lightly destabilizing. Thus, no highly destabilizing mutations are associated with mild phenotypes in males, and residues clearly interacting with microtubules are also less evident.

Finally, in females, milder mutations have a range of predicted effects: the surface residues p.S47N (discussed earlier in the text), p.R78H and p.R102C are predicted to interact with microtubules, p.K134E and p.R196S/H may interact with microtubules; and p.F243S probably does not interact with microtubules. One lightly destabilizing mutation (p.D62N) and several highly destabilizing (p.D62E, p.Y125H, p.V182F, p.R186H, p.R192W and p.I214T) mutations also give milder phenotypes. It should be noted that the X-inactivation status of the majority of these patients is not known; however, p.R192W patients are known to have biased inactivation. Finally, unaffected female carriers, for which X-inactivation status was either non-biased or not known, had the following mutation types: surface and interacting with microtubules (p.K174E but present in a linker), surface and possibly interacting (p.R196C/H), surface and not interacting (p.K193E) and mildly destabilizing (p.T183I). Of note, none of the unaffected female carriers had highly destabilizing mutations.

Discussion

This study presents a mutation analysis in the largest cohort of patients yet reported with sporadic SBH and lissencephaly, and familial lissencephaly–SBH. Fourteen years after the discovery of *DCX*, the aim of our analysis was to provide new insights into the spectrum of phenotypes of patients with *DCX* mutations. We investigated mutation position in the protein, taking into account structural biological data, and compared this with detailed clinical characterizations. Our study examined the clinical and brain MRI characteristics of 136 individuals harbouring 87 *de novo* or inherited mutations in the *DCX* gene, of which 24 mutations are described for the first time here.

The overall information that can be drawn from this study is that (i) the range of CNS involvement is wider than originally described, with a significant proportion of asymptomatic female carriers found to carry *DCX* mutations when their affected son is diagnosed with lissencephaly; (ii) the degree of neurological impairment is related to the band heterotopia thickness and the overlying cortical abnormalities; (iii) skewed X-inactivation plays a role in explaining familial cases of *DCX* with 'severe effect'

Table 4 Comparison of male cases with *DCX* mutations according to severity

	LIS grade 1–2 (diffuse agyria)[a]	LIS grade 3–4 (anterior agyria or pachygyria)[a]	LIS grade 5–6 (SBH +/− pachygyria)	*P*-value
Total	10	24	9	
Age at last evaluation (median [range])	4 years [0.8–24]	12 years [2–37]	5 years [1.5–34]	0.28
Status				<0.001
Inherited mutations (*n* = 29) (%)	4/10 (40)	23/24 (95.8)	2/9 (22.2)	
***De novo* mutations (*n* = 14)** (%)	6/10 (60)	1/24 (4.2)	7/9 (77.8)	
DCX mutation type				0.06
Nonsense and deletion (*n* = 4)	1 *de novo* mutation (1 patient)		3 *de novo* mosaic mutation (3 patient)	
Missense N-DC (*n* = 7)	4 *de novo* mutations (4 patients)	2 inh. mutations (4 patients, 2 families)	1 *de novo* mutation (1 patient)	
Missense C-DC (*n* = 12)	4 *de novo* mutations (4 patients)	4 inh. and 1 *de novo* mutations (9 patients, 7 families)	1 inh and 2 *de novo* mutations (3 patients)	
Missense N terminal domain–interdomain (*n* = 6)	0	4 inh. and 1 *de novo* mutations (9 patients)	1 patient (1 inh. mutation)	
Unclassified (splicing defect *n* = 1, **in-frame deletion *n* = 1)**	1 *de novo* mutation (1 patient)		1 *de novo* mutation (1 patient)	
Disease onset (*n* = 42)				0.004
Prenatal diagnosis (%)	0	1 (4.2)	0	
Developmental delay (%)	1 (11.1)	15 (62.5)	1 (11.1)	
Seizures (including West) (%)	8 (88.9)	8 (33.3)	8 (88.9)	
Microcephaly (%)	8/10 (80)	6/24 (25)	1/9 (11.1)	0.002
Epilepsy (*n* = 42) (%)	10/10 (100)	18/23 (78.3)	9/9 (100)	0.17
Seizure control				0.006
Refractory (%)	8/10 (80)	3/17 (17.6)	6/9 (66.7)	
Partial drug resistance (%)	0	4/17 (23.5)	2/9 (22.2)	
Seizure control (%)	2/10 (20)	10/17 (58.8)	1/9 (11.1)	

[a]The number of the denominator indicates the number of patients in whom specific information was available.
NS = not significant; Inh. = inherited.

mutations, and other atypical situations; (iv) there are several hot spot mutations in *DCX*, explaining collectively 34.5% of cases with SBH, 38.7% of *de novo* mutations and 24% of inherited mutations; (v) varying ratios of classes of mutations (missense in different domains and linkers, nonsense and other) were identified in the different categories of patients, which are also associated with distinct mutations, and phenotype severity can often apparently be correlated with genotype; and (vi) for a subset of mutated surface residues, the substituted amino acid also appears to be critical in determining phenotype severity.

Female patients with subcortical band heterotopia: two distinct groups rather than a continuum

With this large cohort, two groups of female patients with *DCX* mutations clearly emerge: a milder phenotype mainly affecting carrier females compared with a more severe presentation usually observed in sporadic patients. The first group is characterized by either thin frontal bands or mostly normal MRIs. These female carriers are usually diagnosed during their pregnancy or when their affected sons are diagnosed with lissencephaly. The majority of these female carriers (9/10) harbour *de novo DCX* mutations. A few cases of mother–daughter transmission with similar milder forms and non-biased X-inactivation suggest the milder effect of these mutations on DCX function. The occurrence of familial SBH is lower than sporadic SBH cases, representing one-third of the population of females with *DCX* mutation, but we cannot exclude that these patients are underdiagnosed. At the other end of the spectrum, the more frequent (66.7%) and severe presentation is characterized by thicker SBH, combined with moderate to severe intellectual disability, behavioural disturbances and epilepsy, which is often drug resistant. In these cases, severe intellectual impairment, in turn, may cause a reproductive disadvantage, increasing the likelihood for sporadic occurrence.

Similarly, male patients with lissencephaly fall into two groups according to the occurrence of *DCX* mutations, inherited or *de novo*, although the difference is not as striking as for females. Males with lissencephaly and *de novo* mutations are either more severely affected, with a large proportion exhibiting diffuse agyria (more than half in our series), or show a milder SBH phenotype with or without pachygyria (in one-third of patients) and are likely to be mosaics. Thus, males with *de novo* mutations are more severely affected than those with inherited mutations, and are correlated with the involvement of more 'severe effect' mutations (Tables 2 and 4). In contrast, patients with lissencephaly and inherited mutations consistently demonstrate a more moderate phenotype, with anterior agyria (LIS grade 3) or pachygyria (LIS grade 4) in the majority of patients (here, 79.3% of patients).

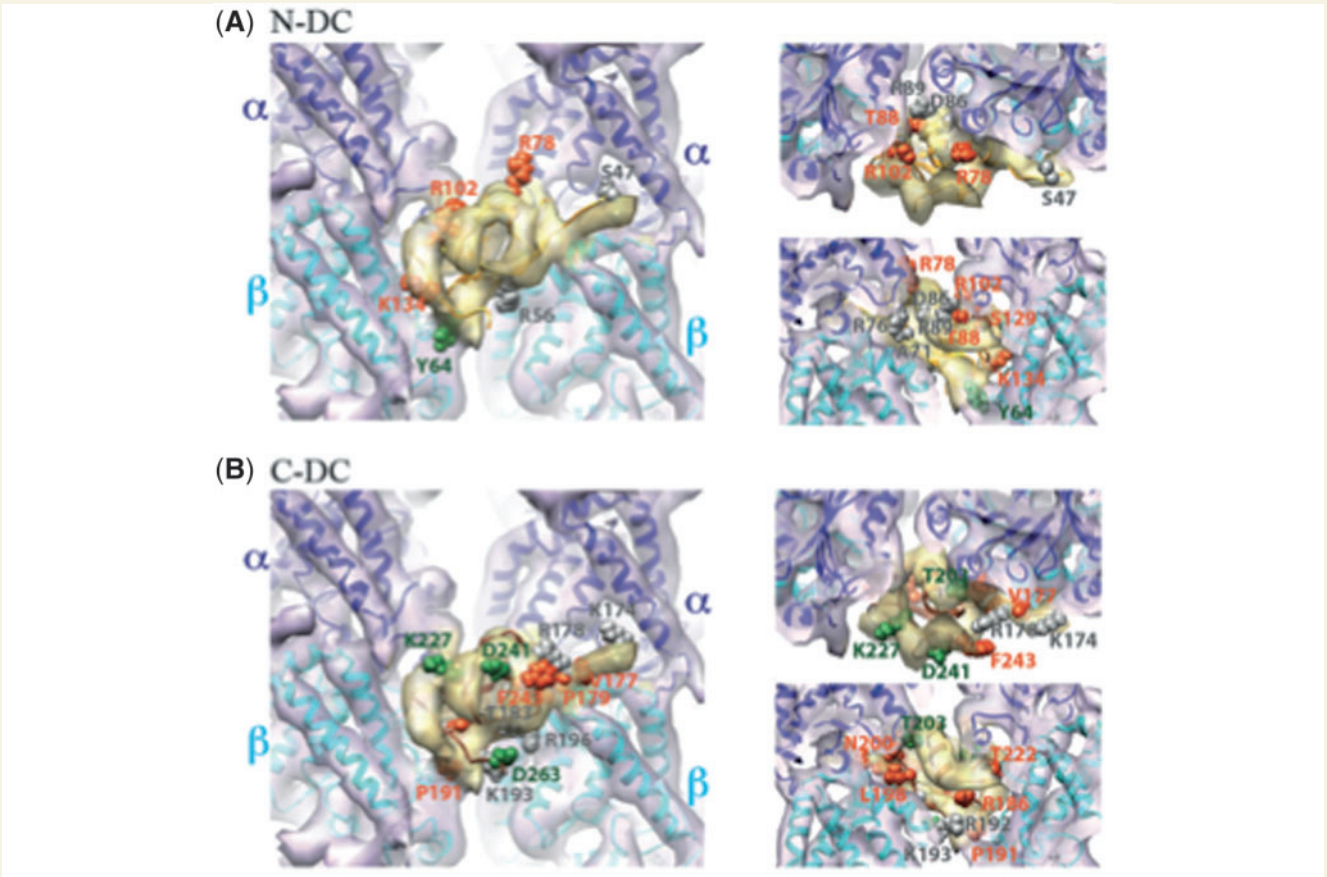

Figure 6 Localization of surface residues mutated in DCX in SBH and their relationship with the microtubule interface. (**A**) Structure of the DCX–microtubule interface [cryo-electron microscopy reconstruction displayed as a transparent surface, tubulin in purple, DCX in yellow; EMDB ID 1788 (Kim *et al*., 2003; Fourniol *et al*., 2010)] docked with the pseudo-atomic structure of the N-DC–microtubule interface [ribbons, α-tubulin in blue, β-tubulin in cyan, N-DC in orange; PDB ID 2XRP (Kim *et al*., 2003; Fourniol *et al*., 2010)]. *Left*: front view; *top right*: view from the microtubule plus end; *bottom right*: view from the centre of the microtubule outwards. N-DC surface residues subject to missense mutations are displayed as spheres, coloured in green for cases with absence of cortex malformations (R102, K134), grey for mild/moderate phenotypes (S47), and orange for severe cases (R59, Y64, R76, R78, S129). Note that when a mutation resulted in more or less severe SBH in different patients, the most severe phenotype was considered in this figure. (**B**) Same as in **A** but docked with a homology model of C-DC (ribbons, brown). Green spheres: surface residue, the mutation of which resulted in an absence of phenotype (K193; however, X-inactivation status for the individual with this mutation is not available, and this residue results in a severe phenotype in a male with lissencephaly); grey spheres: surface residues the mutation of which caused milder SBH (K174, T183, R196, T203, K227, F243 and D263); orange: severe SBH cases (V177, P179, R186, R192, L198 and D241). Of note, milder-effect mutations apparently appear more frequently in C-DC than in N-DC.

The band thickness determines the neurological phenotype in female patients with *DCX* mutations

Previous work, which did not involve genetic analysis, has underlined the importance of band thickness in the outcome of patients with SBH in a series not studied at the genetic level (Palmini *et al*., 1991; Barkovich *et al*., 1994). Following this seminal work, genetic data have thus far contributed to the identification of three SBH genes: (i) *DCX* that accounts for 100% of familial cases, and 53 to 80% of sporadic cases; (ii) mosaic mutations of *LIS1* (Sicca *et al*., 2003); and (iii) mutations in *TUBA1A* (Poirier *et al*., 2007) accounting for some further rare cases. Here, with a large cohort of 136 patients with confirmed *DCX* mutations and detailed clinical and radiological data, we confirm the predictive value of band thickness. According to previous data, four categories were defined, from the mildest (grade 1), characterized by a thin band restricted to the frontal lobes, to the most severe (grade 4), characterized by a thick and complete band around the entire cerebrum, the thinnest part being in the temporal and occipital lobes. Although this segmentation represents an interesting predictive tool in late childhood and adulthood, our data demonstrate that in young patients, band thickness is difficult to determine. Here, 12 sporadic patients aged <2 years had T_1-weighted images close to the lissencephaly pattern, while T_2 images showed the heterotopic band. This change in cortical thickness according

to age is reminiscent of the changing aspect described in polymicrogyria (Takanashi and Barkovich, 2003). Although serial images were not performed in these patients, this pattern does not seem to represent a difference in morphology but rather changes in the maturity of the cortex and underlying white matter. In clinical practice, the distinction of two categories is convenient. Thicker SBH (>8 mm) is the most frequent presentation of SBH (61.4% in accordance with the Barkovich series, 62.9%) (Barkovich *et al.*, 1994) and more specifically in sporadic patients (81.9%). Thicker bands are more frequently associated with frontal pachygyria, with shallow to very shallow sulci, moderate to severe ventricular enlargement and prominent perivascular spaces in subcortical or periventricular regions, when compared with patients with thin SBH (<8 mm). This suggests that the neuronal arrest that leads to the formation of the band is also likely to impair the development of cortical gyri and cerebral white matter. This has previously been suggested in periventricular heterotopia (Hannan *et al.*, 1999; Ferland *et al.*, 2009) and in SBH animal models (Ackman *et al.*, 2009; Croquelois *et al.*, 2009). Thicker bands lead to more severe intellectual impairment, and more behavioural disturbances and are also responsible for polymorphic epileptic seizures, usually of the Lennox–Gastaut syndrome type, with earlier age of onset and showing more resistance to anti-epileptic drugs.

In lissencephaly, our previous study found that the majority of male patients with *DCX* mutations displayed either a LIS grade 3 or 4 (i.e. anterior agyria or pachygyria). Similar to SBH, the severity of neurological impairment in lissencephaly is determined by the degree of agyria (Dobyns *et al.*, 1992). Here with a larger cohort, our data reinforce these results, with 53.5% patients showing LIS grade 3 or 4. More importantly, our present results confirm previous data, suggesting that the LIS grade is less severe in inherited *DCX* mutations compared with those with *de novo* mutations (Leger *et al.*, 2008). This suggests that *de novo* mutations may have a more severe effect on *DCX* function.

Little is known about the connectivity and function of heterotopic neurons. Although the band has a disorganized disposition of pyramidal cells, there is evidence that connectivity within the band, and with normal cortical or subcortical neurons, is maintained (Palmini *et al.*, 1991). The functional role of this double cortex has not yet been completely clarified even if functional MRI, PET and diffusion tensor imaging have contributed in part to understanding the neurophysiology. By depth electrode recordings, nerve cells within the SBH have been shown to exhibit epileptiform activity similar to and synchronous with those observed in the overlying cortex (De Volder *et al.*, 1994; Pinard *et al.*, 2000; Spreer *et al.*, 2001). Electrophysiological data with electrocorticography–functional MRI (Tyvaert *et al.*, 2008) and an SBH rat model (Ackman *et al.*, 2009; Lapray *et al.*, 2010) show that both heterotopia and the overlying cortex contribute to epileptic manifestations. Hence, major alterations not only affect the neurons that fail to migrate but also their programmed target areas. Altogether, these data suggest that despite integration of the heterotopia into networks, the more severe clinical phenotypes associated with thicker bands lead to appreciable abnormal functioning of either the lesion or the overlying cortex, or both.

Proposed mechanisms for phenotypic heterogeneity in subcortical band heterotopia

In SBH, one population of neurons forms a relatively normal cortex, whereas a second population apparently arrests during migration leading to a collection of neurons beneath the cortex. Because SBH is predominantly an X-linked disorder, the phenotype of females is thought to result from a mosaic state due to X-inactivation in which neurons express either a normal or a mutant copy of *DCX*. Previous data suggest that somatic mosaicism can produce the same result (Gleeson *et al.*, 2000; Aigner *et al.*, 2003). A third possibility might be the influence of milder mutations.

Some previous studies suggest that skewed X-inactivation does not significantly contribute to the SBH phenotype (Demelas *et al.*, 2001; Matsumoto *et al.*, 2001). Here, we found a significant proportion of skewed X-inactivation cases in carrier females (37.5%) in accordance with results from one smaller series (Guerrini *et al.*, 2003). In contrast, skewed X-inactivation is rarer (14.7%) in SBH cases with *de novo DCX* mutations. This suggests that a biased inactivation may partially account for phenotypic variability at least for familial cases. In support of this, skewed X-inactivation may explain phenotypic heterogeneity between familial and sporadic patients with the same mutations. This situation was found in mildly symptomatic female carriers with biased inactivation and two more severely affected sporadic patients, all carrying the same mutation, p.R192W. Analogously for the only nonsense mutation p.R272X found in familial and sporadic cases, skewed X-inactivation found in the carrier female is likely to explain her milder phenotype, while others have reported thick heterotopic bands with balanced X-inactivation (Gleeson *et al.*, 1998; Matsumoto *et al.*, 2001). Of note, this observation of the same mutation in both *de novo* and inherited cases is extremely rare in the literature and in our series. Also it is noteworthy that variable degrees of X-inactivation were observed in similarly affected patients with recurrent mutations (i.e. p.R196H and p.D9N), suggesting that other mechanisms may account for these less severe presentations, including a milder effect of these mutations on protein function. Altogether, these results suggest that although skewing of X-inactivation may play a significant role in phenotypic heterogeneity, it ultimately is not demonstrated in all cases.

Somatic and germline mosaicisms associated with phenotypic heterogeneity in SBH were previously found in 10% of unaffected mothers whose children presented with either SBH or lissencephaly (Gleeson *et al.*, 2000*b*; Aigner *et al.*, 2003). Several authors suggest that there may be a critical percentage of mosaicism in peripheral blood that is associated with phenotypic features of SBH (Gleeson *et al.*, 2000*b*; Kato *et al.*, 2001; Poolos *et al.*, 2002). With <30% mosaicism, patients are clinically unaffected, whereas those with >30% mosaicism are symptomatic with SBH. In our cohort, mosaicism of <30% was found in three males with *de novo* nonsense mutations and an exonic deletion of *DCX*. This naturally leads to milder phenotypes with SBH in all three cases. Intriguingly, mosaic mutations were suspected but not

demonstrated in blood lymphocytes of several familial cases (here, Families 25 and 11) in which both mothers were clearly asymptomatic, had one of two children including females, with a severe phenotype, i.e. SBH grade 4. The possibility of somatic mosaicism in neural cells in these cases cannot be ruled out.

DCX mutations: is there a genotype–phenotype correlation for lissencephaly and subcortical band heterotopia?

To better understand the pathophysiological basis for the dichotomy between patients with *de novo DCX* mutations and inherited mutations, and to provide further proof of the phenotypic effect of the mutations, we analysed mutation type and location and searched for genotype–phenotype correlations. Our data clearly show that a correlation does exist in these *DCX*-related conditions, in both SBH and lissencephaly. This is supported by the similar phenotypes associated with recurrent mutations. For example, the most frequent substitution of the C-DC surface residue Arg196 (24% of inherited DCX mutations) is consistently associated with less severe SBH, either poorly symptomatic or asymptomatic female carriers, or in affected males with lissencephaly with a milder presentation. This recurrent mutation was never previously reported to be a hot spot, reflecting probably different ethnic origins of our population and those previously reported. Other recurrent mutations are strongly associated with severe SBH. Of these, the substitutions of Arg186, accounting for 20.9% of *de novo DCX* mutations in our series, invariably result in severe forms. Interestingly, structural predictions suggest that this residue is crucial for the stability of C-DC, with mutations at Arg59 in N-DC having a similar effect.

On the other hand, some missense mutations of the same residue (e.g. p.R78L/H/C) have variable consequences. R78 is predicted to be in a loop of N-DC that participates in microtubule binding. In this case, it is likely that the severity of the phenotype is related to the substituted residue. The mutation p.R78H, associated with a milder phenotype, is predicted to have less of an effect on the charge of the side chain that contacts tubulin, whereas the substitutions p.R78L and p.R78C, associated with more severe phenotypes, are likely to more strongly impair the interaction with microtubules.

While nonsense mutations are spread throughout the *DCX* gene, missense mutations are clustered in N-DC and C-DC, supporting the significance of these two domains for DCX function. However, the variable severity among patients with SBH was not correlated with a particular distribution of mutations in either the N-DC or C-DC domains. By separating mutations according to their predicted consequences on DCX structure or ability to bind microtubules, we found that highly destabilizing mutations, in general, tend to give more severe phenotypes. It is noteworthy that this type of mutation is observed less frequently in males, further reinforcing their potential detrimental consequences on DCX. Thus, structural data provide insights to predict phenotype severity. Moreover, some severe surface mutations in females (p.R78C/L) and in males (p.Y64N), which do not destabilize the protein, are predicted to be in direct contact with microtubules, and presumably lead to a critical loss of function. On the other hand, other mutations potentially affecting microtubule interaction led to less severe effects (p.S47N, p.R76S, p.R78H, p.R102C, p.K134E and p.R196C/S/H), perhaps only reducing affinity of interaction due to their position or the substituted residue. Other residues facing away from the microtubule interface (e.g. p.K193E) presumably are important for other partner interactions. Clinical data thus also contribute to the identification of such residues and the fine analysis of DCX's function.

Concerning different types of *DCX* mutations, it is noteworthy that only 5 of 93 females with SBH were found to carry an intragenic deletion or duplication of the *DCX* gene. This result contrasts with previous results (Mei *et al*. 2007; Haverfield *et al*. 2009), describing the presence of *DCX* intragenic deletions/duplications in about one-third of their patients with SBH, and we currently do not have explanations for this difference.

Both N-DC and C-DC play a major role in the function of *DCX*

Although most structural studies to date have focused on the N-DC domain (Kim *et al*., 2003; Fourniol *et al*., 2010), our analyses reinforce the idea that both DC domains are important for the full functionality of DCX (Horesh *et al*., 1999; Taylor *et al*., 2000). For the purposes of our current analysis, we assumed that N-DC and C-DC make equivalent contacts with microtubules, although since C-DC can bind tubulin heterodimers (Taylor *et al*., 2000; Kim *et al*., 2003) as well as microtubules and other partners, it may play additional roles to N-DC. Individual mutations occur in N- and C-DC with similar frequencies, although recurrent mutations increase the overall number in C-DC. Thus, the C-DC domain is clearly essential for microtubule-related and other functions of DCX. Further correlations of structural predictions of mutations with phenotype in the future will continue to help elucidate the functions of DCX.

Conclusion

Taken as a whole, these observations demonstrate that *DCX*-related disorders represent a clinically heterogeneous syndrome. In females with SBH, two groups clearly emerge, with a milder form mainly affecting carrier females that are potentially underdiagnosed and a more severe and frequent presentation usually observed in sporadic patients. Hot spot mutations are more prevalent than previously reported. Radiological and clinical data combined with structural data point to the fact that it is possible to make genotype–phenotype correlations taking into account X-inactivation status, the residue affected by the mutation, the likelihood of the mutation to destabilize the protein, and in the case of surface residues, the substituting amino acid.

Funding

We are grateful for financial support from the Agence National de Recherche (ANR-08-MNP-013; F.F. and N.B.B., ANR 2010-Blanc

1103 01; J.C.), as well as from INSERM, including the Avenir program (F.F.), the Fondation Bettencourt Schueller (F.F.), the Fédération pour la recherche sur le cerveau (FRC for F.F. and A.H.), the FRM (Equipe FRM 2007 to J.C.) and ANR-Eranet-Erare. F.J.F. and C.A.M. were supported by The Wellcome Trust and New Life.

Supplementary material

Supplementary material is available at *Brain* online.

References

Abdollahi MR, Morrison E, Sirey T, Molnar Z, Hayward BE, Carr IM, et al. Mutation of the variant alpha-tubulin TUBA8 results in polymicrogyria with optic nerve hypoplasia. Am J Hum Genet 2009; 85: 737–44.

Ackman JB, Aniksztejn L, Crepel V, Becq H, Pellegrino C, Cardoso C, et al. Abnormal network activity in a targeted genetic model of human double cortex. J Neurosci 2009; 29: 313–27.

Aigner L, Fluegel D, Dietrich J, Ploetz S, Winkler J. Isolated lissencephaly sequence and double-cortex syndrome in a German family with a novel doublecortin mutation. Neuropediatrics 2000; 31: 195–8.

Aigner L, Uyanik G, Couillard-Despres S, Ploetz S, Wolff G, Morris-Rosendahl D, et al. Somatic mosaicism and variable penetrance in doublecortin-associated migration disorders. Neurology 2003; 60: 329–32.

Barkovich AJ, Guerrini R, Battaglia G, Kalifa G, N'Guyen T, Parmeggiani A, et al. Band heterotopia: correlation of outcome with magnetic resonance imaging parameters. Ann Neurol 1994; 36: 609–17.

Barkovich AJ, Jackson DE Jr, Boyer RS. Band heterotopias: a newly recognized neuronal migration anomaly. Radiology 1989; 171: 455–8.

Berg AT, Berkovic SF, Brodie MJ, Buchhalter J, Cross JH, van Emde Boas W, et al. Revised terminology and concepts for organization of seizures and epilepsies: report of the ILAE Commission on Classification and Terminology, 2005-2009. Epilepsia 2010; 51: 676–85.

Caspi M, Atlas R, Kantor A, Sapir T, Reiner O. Interaction between LIS1 and doublecortin, two lissencephaly gene products. Hum Mol Genet 2000; 9: 2205–13.

Collins DW, Jukes TH. Rates of transition and transversion in coding sequences since the human-rodent divergence. Genomics 1994; 20: 386–96.

Croquelois A, Giuliani F, Savary C, Kielar M, Amiot C, Schenk F, et al. Characterization of the HeCo mutant mouse: a new model of subcortical band heterotopia associated with seizures and behavioral deficits. Cereb Cortex 2009; 19: 563–75.

Demelas L, Serra G, Conti M, Achene A, Mastropaolo C, Matsumoto N, et al. Incomplete penetrance with normal MRI in a woman with germline mutation of the DCX gene. Neurology 2001; 57: 327–30.

De Volder AG, Gadisseux JF, Michel CJ, Maloteaux JM, Bol AC, Grandin CB, et al. Brain glucose utilization in band heterotopia: synaptic activity of 'double cortex'. Pediatr Neurol 1994; 11: 290–4.

des Portes V, Pinard JM, Billuart P, Vinet MC, Koulakoff A, Carrie A, et al. A novel CNS gene required for neuronal migration and involved in X-linked subcortical laminar heterotopia and lissencephaly syndrome. Cell 1998a; 92: 51–61.

des Portes V, Francis F, Pinard JM, Desguerre I, Moutard ML, Snoeck I, et al. Doublecortin is the major gene causing X-linked subcortical laminar heterotopia (SCLH). Hum Mol Genet 1998b; 7: 1063–70.

Dobyns WB, Andermann E, Andermann F, Czapansky-Beilman D, Dubeau F, Dulac O, et al. X-linked malformations of neuronal migration. Neurology 1996; 47: 331–9.

Dobyns WB, Berry-Kravis E, Havernick NJ, Holden KR, Viskochil D. X-linked lissencephaly with absent corpus callosum and ambiguous genitalia. Am J Med Genet 1999b; 86: 331–7.

Dobyns WB, Elias ER, Newlin AC, Pagon RA, Ledbetter DH. Causal heterogeneity in isolated lissencephaly. Neurology 1992; 42: 1375–88.

Dobyns WB, Truwit CL. Lissencephaly and other malformations of cortical development: 1995 update. Neuropediatrics 1995; 26: 132–47.

Dobyns WB, Truwit CL, Ross ME, Matsumoto N, Pilz DT, Ledbetter DH, et al. Differences in the gyral pattern distinguish chromosome 17-linked and X-linked lissencephaly. Neurology 1999a; 53: 270–7.

Ferland RJ, Batiz LF, Neal J, Lian G, Bundock E, Lu J, et al. Disruption of neural progenitors along the ventricular and subventricular zones in periventricular heterotopia. Hum Mol Genet 2009; 18: 497–516.

Fourniol FJ, Sindelar CV, Amigues B, Clare DK, Thomas G, Perderiset M, et al. Template-free 13-protofilament microtubule-MAP assembly visualized at 8 A resolution. J Cell Biol 2010; 191: 463–70.

Francis F, Koulakoff A, Boucher D, Chafey P, Schaar B, Vinet MC, et al. Doublecortin is a developmentally regulated, microtubule-associated protein expressed in migrating and differentiating neurons. Neuron 1999; 23: 247–56.

Friocourt G, Kappeler C, Saillour Y, Fauchereau F, Rodriguez MS, Bahi N, et al. Doublecortin interacts with the ubiquitin protease DFFRX, which associates with microtubules in neuronal processes. Mol Cell Neurosci 2005; 28: 153–64.

Gleeson JG, Lin PT, Flanagan LA, Walsh CA. Doublecortin is a microtubule-associated protein and is expressed widely by migrating neurons. Neuron 1999b; 23: 257–71.

Gleeson JG, Luo RF, Grant PE, Guerrini R, Huttenlocher PR, Berg MJ, et al. Genetic and neuroradiological heterogeneity of double cortex syndrome. Ann Neurol 2000a; 47: 265–9.

Gleeson JG, Minnerath S, Kuzniecky RI, Dobyns WB, Young ID, Ross ME, et al. Somatic and germline mosaic mutations in the doublecortin gene are associated with variable phenotypes. Am J Hum Genet 2000b; 67: 574–81.

Gleeson JG, Minnerath SR, Fox JW, Allen KM, Luo RF, Hong SE, et al. Characterization of mutations in the gene doublecortin in patients with double cortex syndrome. Ann Neurol 1999a; 45: 146–53.

Gleeson JG, Allen KM, Fox JW, Lamperti ED, Berkovic S, Scheffer I, et al. Doublecortin, a brain-specific gene mutated in human X-linked lissencephaly and double cortex syndrome, encodes a putative signaling protein. Cell 1998; 92: 63–72.

Guerrini R, Moro F, Andermann E, Hughes E, D'Agostino D, Carrozzo R, et al. Nonsyndromic mental retardation and cryptogenic epilepsy in women with doublecortin gene mutations. Ann Neurol 2003; 54: 30–7.

Hannan AJ, Servotte S, Katsnelson A, Sisodiya S, Blakemore C, Squier M, et al. Characterization of nodular neuronal heterotopia in children. Brain 1999; 122 (Pt 2): 219–38.

Haverfield EV, Whited AJ, Petras KS, Dobyns WB, Das S. Intragenic deletions and duplications of the LIS1 and DCX genes: a major disease-causing mechanism in lissencephaly and subcortical band heterotopia. Eur J Hum Genet 2009; 17: 911–8.

Horesh D, Sapir T, Francis F, Wolf SG, Caspi M, Elbaum M, et al. Doublecortin, a stabilizer of microtubules. Hum Mol Genet 1999; 8: 1599–610.

Jaglin XH, Poirier K, Saillour Y, Buhler E, Tian G, Bahi-Buisson N, et al. Mutations in the beta-tubulin gene TUBB2B result in asymmetrical polymicrogyria. Nat Genet 2009; 41: 746–52.

Kappeler C, Saillour Y, Baudoin JP, Tuy FP, Alvarez C, Houbron C, et al. Branching and nucleokinesis defects in migrating interneurons derived from doublecortin knockout mice. Hum Mol Genet 2006; 15: 1387–400.

Kato M, Kanai M, Soma O, Takusa Y, Kimura T, Numakura C, et al. Mutation of the doublecortin gene in male patients with double cortex syndrome: somatic mosaicism detected by hair root analysis. Ann Neurol 2001; 50: 547–51.

Keays DA, Tian G, Poirier K, Huang GJ, Siebold C, Cleak J, et al. Mutations in alpha-tubulin cause abnormal neuronal migration in mice and lissencephaly in humans. Cell 2007; 128: 45–57.

Kim MH, Cierpicki T, Derewenda U, Krowarsch D, Feng Y, Devedjiev Y, et al. The DCX-domain tandems of doublecortin and doublecortin-like kinase. Nat Struct Biol 2003; 10: 324–33.

Kizhatil K, Wu YX, Sen A, Bennett V. A new activity of doublecortin in recognition of the phospho-'QY tyrosine in the cytoplasmic domain of neurofascin. J Neurosci 2002; 22: 7948–58.

Koizumi H, Higginbotham H, Poon T, Tanaka T, Brinkman BC, Gleeson JG. Doublecortin maintains bipolar shape and nuclear translocation during migration in the adult forebrain. Nat Neurosci 2006; 9: 779–86.

Lapray D, Popova IY, Kindler J, Jorquera I, Becq H, Manent JB, et al. Spontaneous epileptic manifestations in a DCX knockdown model of human double cortex. Cereb Cortex 2010; 20: 2694–701.

Leger PL, Souville I, Boddaert N, Elie C, Pinard JM, Plouin P, et al. The location of DCX mutations predicts malformation severity in X-linked lissencephaly. Neurogenetics 2008; 9: 277–85.

Lo Nigro C, Chong CS, Smith AC, Dobyns WB, Carrozzo R, Ledbetter DH. Point mutations and an intragenic deletion in LIS1, the lissencephaly causative gene in isolated lissencephaly sequence and Miller-Dieker syndrome. Hum Mol Genet 1997; 6: 157–64.

Matsumoto N, Leventer RJ, Kuc JA, Mewborn SK, Dudlicek LL, Ramocki MB, et al. Mutation analysis of the DCX gene and genotype/phenotype correlation in subcortical band heterotopia. Eur J Hum Genet 2001; 9: 5–12.

Mei D, Parrini E, Pasqualetti M, Tortorella G, Franzoni E, Giussani U, et al. Multiplex ligation-dependent probe amplification detects DCX gene deletions in band heterotopia. Neurology 2007; 68: 446–50.

Monteiro J, Derom C, Vlietinck R, Kohn N, Lesser M, Gregersen PK. Commitment to X inactivation precedes the twinning event in monochorionic MZ twins. Am J Hum Genet 1998; 63: 339–46.

Moores CA, Perderiset M, Francis F, Chelly J, Houdusse A, Milligan RA. Mechanism of microtubule stabilization by doublecortin. Mol Cell 2004; 14: 833–9.

Moores CA, Perderiset M, Kappeler C, Kain S, Drummond D, Perkins SJ, et al. Distinct roles of doublecortin modulating the microtubule cytoskeleton. EMBO J 2006; 25: 4448–57.

Palmini A, Andermann F, Aicardi J, Dulac O, Chaves F, Ponsot G, et al. Diffuse cortical dysplasia, or the 'double cortex' syndrome: the clinical and epileptic spectrum in 10 patients. Neurology 1991; 41: 1656–62.

Pettersen EF, Goddard TD, Huang CC, Couch GS, Greenblatt DM, Meng EC, et al. UCSF Chimera—a visualization system for exploratory research and analysis. J Comput Chem 2004; 25: 1605–12.

Pilz DT, Kuc J, Matsumoto N, Bodurtha J, Bernadi B, Tassinari CA, et al. Subcortical band heterotopia in rare affected males can be caused by missense mutations in DCX (XLIS) or LIS1. Hum Mol Genet 1999; 8: 1757–60.

Pilz DT, Matsumoto N, Minnerath S, Mills P, Gleeson JG, Allen KM, et al. LIS1 and XLIS (DCX) mutations cause most classical lissencephaly, but different patterns of malformation. Hum Mol Genet 1998; 7: 2029–37.

Pinard J, Feydy A, Carlier R, Perez N, Pierot L, Burnod Y. Functional MRI in double cortex: functionality of heterotopia. Neurology 2000; 54: 1531–3.

Poirier K, Keays DA, Francis F, Saillour Y, Bahi N, Manouvrier S, et al. Large spectrum of lissencephaly and pachygyria phenotypes resulting from de novo missense mutations in tubulin alpha 1A (TUBA1A). Hum Mutat 2007; 28: 1055–64.

Poirier K, Saillour Y, Bahi-Buisson N, Jaglin XH, Fallet-Bianco C, Nabbout R, et al. Mutations in the neuronal {beta}-tubulin subunit TUBB3 result in malformation of cortical development and neuronal migration defects. Hum Mol Genet 2010; 19: 4462–73.

Poolos NP, Das S, Clark GD, Lardizabal D, Noebels JL, Wyllie E, et al. Males with epilepsy, complete subcortical band heterotopia, and somatic mosaicism for DCX. Neurology 2002; 58: 1559–62.

Reiner O, Carrozzo R, Shen Y, Wehnert M, Faustinella F, Dobyns WB, et al. Isolation of a Miller-Dieker lissencephaly gene containing G protein beta-subunit-like repeats. Nature 1993; 364: 717–21.

Sali A, Blundell TL. Comparative protein modelling by satisfaction of spatial restraints. J Mol Biol 1993; 234: 779–815.

Sapir T, Horesh D, Caspi M, Atlas R, Burgess HA, Wolf SG, et al. Doublecortin mutations cluster in evolutionarily conserved functional domains. Hum Mol Genet 2000; 9: 703–12.

Schaar BT, Kinoshita K, McConnell SK. Doublecortin microtubule affinity is regulated by a balance of kinase and phosphatase activity at the leading edge of migrating neurons. Neuron 2004; 41: 203–13.

Sicca F, Kelemen A, Genton P, Das S, Mei D, Moro F, et al. Mosaic mutations of the LIS1 gene cause subcortical band heterotopia. Neurology 2003; 61: 1042–6.

Spreer J, Martin P, Greenlee MW, Wohlfarth R, Hammen A, Arnold SM, et al. Functional MRI in patients with band heterotopia. Neuroimage 2001; 14: 357–65.

Taylor KR, Holzer AK, Bazan JF, Walsh CA, Gleeson JG. Patient mutations in doublecortin define a repeated tubulin-binding domain. J Biol Chem 2000; 275: 34442–50.

Takanashi J, Barkovich AJ. The changing MR imaging appearance of polymicrogyria: a consequence of myelination. AJNR Am J Neuroradiol 2003; 24: 788–93.

Tilney LG, Hatano S, Ishikawa H, Mooseker MS. The polymerization of actin: its role in the generation of the acrosomal process of certain echinoderm sperm. J Cell Biol 1973; 59: 109–26.

Tischfield MA, Baris HN, Wu C, Rudolph G, Van Maldergem L, He W, et al. Human TUBB3 mutations perturb microtubule dynamics, kinesin interactions, and axon guidance. Cell 2010; 140: 74–87.

Tsukada M, Prokscha A, Oldekamp J, Eichele G. Identification of neurabin II as a novel doublecortin interacting protein. Mech Dev 2003; 120: 1033–43.

Tyvaert L, Hawco C, Kobayashi E, LeVan P, Dubeau F, Gotman J. Different structures involved during ictal and interictal epileptic activity in malformations of cortical development: an EEG-fMRI study. Brain 2008; 131 (Pt 8): 2042–60.

Appendix 1

SBH-LIS European consortium: Cecilia Altuzarra (CHU Besançon), Isabelle An (Pitié Salpétrière, APHP Paris), Alexis Arzimanoglou (HFME-CHU Lyon), Sandrine Aubert (La Timone, APHM, Marseille), Stéphane Auvin (Robert Debré, APHP Paris), Marie-Anne Barthez (CHU Tours), Daniella Bartholdi (CH Zurich-Suisse), Fabrice Bartholomei (La Timone, APHM, Marseille), Arnaud Biraben (CHU Rennes), Viviane Bouilleret (Bicètre APHP, Paris), Lorene Bouillot (HFME-CHU Lyon), Odile Boute (CHU Lille), Thierry Billiar (CH Valenciennes), Marilyn Carneiro (CHU Montpellier), Aude Charollais (CHU Rouen), Jean Marie Cuisset (CHU Lille), Marie Denuelle (CHU Toulouse), Isabelle Desguerre (Necker APHP, Paris), Vincent des Portes (HFME-CHU Lyon), Diane Doummar (Trousseau, APHP, Paris), Patrick Edery (HFME-CHU Lyon), Nouha Essid (Garches, APHP), Valérie Drouin Garaud (CHU Rouen), Agnès Gauthier (CHU Nantes), Sebastien Gay (CHR Macon), Bertrand Isidor (CHU Nantes), Sylvie Joriot (CHU Lille), Sophie Julia (CHU Toulouse), Anna Kaminska (Necker APHP, Paris), Jacques Motte (CHU Reims), Marie Laure Moutard (Trousseau, APHP, Paris), Alice Goldenberg (CHU Rouen), Marie Ange N'Guyen Morel (CHU Grenoble), Cecile Laroche (CHU Limoges), Karine Lascelles (Guys Hospital, UK), Dorit Lev (Wolfson Medical Center, Israel), Marie Dominique Lamblin (CHU Lille), Cecile Laroche (CHU Limoges), Jean Marie Lepage

(CHU Rennes), Jean-Marc Pinard (Garches, APHP, Paris), Serge Rivera (CHU Bayonne), Pascal Sabouraud (CHU Reims), Catherine Sarret (CHU Clermont Ferrant), Bertrand Sotos (CH Troyes), Sylvie Sukno (CHU Lille), Bertrand de Toffol (CHU Tours), Annick Toutain (CHU Tours), Valerie Trommsdorff (CHU La Reunion), Dorothée Ville (HFME-CHU Lyon), Catherine Vincent-Delorme (CHU Lille).